

**Best  
Available  
Copy**

AD-760 127

RESEARCH FOR DETERMINING PROPAGATION  
CHARACTERISTICS OVER ARPA'S NORWEGIAN  
ARRAY. PART II

Mark Landisman

Texas University

Prepared for:

Air Force Cambridge Research Laboratories

February 1973

DISTRIBUTED BY:

**NTIS**

National Technical Information Service  
U. S. DEPARTMENT OF COMMERCE  
5285 Port Royal Road, Springfield Va. 22151

AD 760127

RESEARCH FOR DETERMINING PROPAGATION CHARACTERISTICS  
OVER ARPA'S NORWEGIAN ARRAY

by

Mark Landisman

The University of Texas at Dallas  
P. O. Box 30365  
Dallas, Texas 75230

Contract No. F19628-70-C-0176  
Line Item 2  
Project No. 5130

FINAL REPORT

15 January 1970 - 28 February 1973

February 1973

D D C  
RECEIVED  
MAY 18 1973  
RECEIVED

The views and conclusions contained in this document are those of the authors and should not be interpreted as necessarily representing the official policies, either expressed or implied, of the Advanced Research Projects Agency or the U. S. Government.

Contract Monitor: Emmanuel E. Bliamptis  
Terrestrial Sciences Laboratory

This document has been approved for public release and sale; its distribution is unlimited.

Sponsored by  
Advanced Research Projects Agency  
ARPA Order No. 292  
Monitored by  
AIR FORCE CAMBRIDGE RESEARCH LABORATORIES  
AIR FORCE SYSTEMS COMMAND  
UNITED STATES AIR FORCE  
BEDFORD, MASSACHUSETTS 01730

Reproduced by  
NATIONAL TECHNICAL  
INFORMATION SERVICE  
U S Department of Commerce  
Springfield VA 22151

51

Program Code No.....9F10  
Effective Date of Contract .....6 July 1972  
Contract Expiration Date .....28 February 1973  
Principal Investigator and Phone No.....Mark Landisman  
214-231-1471  
Project Scientist or Engineer and Phone No.....E. E. Sliamptis  
617-861-3662

Qualified requestors may obtain additional copies from the Defense Documentation Center. All others should apply to the National Technical Information Service.

ACCESSION BY	
NTIS	WHIT T. HIGGINS <input checked="" type="checkbox"/>
DOC	DAVE S. GIBSON <input type="checkbox"/>
UNANNOUNCED	<input type="checkbox"/>
JUSTIFICATION	
BY	
DISSEMINATION/AVAILABILITY CODES	
DECL.	AVAIL. 17/8 2. 11/8
A	

ERRATA  
RESEARCH FOR DETERMINING PROPAGATION CHARACTERISTICS  
OVER ARPA'S NORWEGIAN ARRAY

by

Mark Landisman

The University of Texas at Dallas  
P. O. Box 30365  
Dallas, Texas 75230

Contract No. F19628-70-C-0176  
Project No. 5130

FINAL REPORT (Part II)

15 January 1970 - 28 February 1973  
February 1973

Contract Monitor: Emmanuel E. Bliamptis  
Terrestrial Sciences Laboratory

Approved for public release; distribution unlimited.

Sponsored by  
Advanced Research Projects Agency  
ARPA Order No. 292  
Monitored by  
AIR FORCE CAMBRIDGE RESEARCH LABORATORIES  
AIR FORCE SYSTEMS COMMAND  
UNITED STATES AIR FORCE  
BEDFORD, MASSACHUSETTS 01730

ARPA Order No. 292

Program Code No. 9F10

Contractor: University of Texas  
at Dallas

Effective Date of Contract:  
6 July 1972

Contract No. F19628-70-C-0176

Principal Investigator and Phone No.  
Dr. Mark Landisman/214 231-1471

AFCRL Project Scientist and Phone No.  
Emmanuel E. Bliamptis/617 861-3665

Contract Expiration Date:  
28 February 1973

Qualified requestors may obtain additional copies from the Defense Documentation Center. All others should apply to the National Technical Information Service.

RESEARCH FOR DETERMINING PROPAGATION CHARACTERISTICS  
OVER ARPA'S NORWEGIAN ARRAY

by

Mark Landisman

The University of Texas at Dallas  
P. O. Box 30365  
Dallas, Texas 75230

Contract No. F19628-70-C-0176  
Line Item 2  
Project No. 5130

FINAL REPORT

15 January 1970 - 28 February 1973

February 1973

The views and conclusions contained in this document are those of the authors and should not be interpreted as necessarily representing the official policies, either express or implied, of the Advanced Research Projects Agency or the U.S. Government.

Contract Monitor: Emmanuel E. Bliamptis  
Terrestrial Sciences Laboratory

This document has been approved for public release and sale; its distribution is unlimited.

Sponsored by  
Advanced Research Projects Agency  
ARPA Order No. 292  
Monitored by  
AIR FORCE CAMBRIDGE RESEARCH LABORATORIES  
AIR FORCE SYSTEMS COMMAND  
UNITED STATES AIR FORCE  
BEDFORD, MASSACHUSETTS 01730

1-A

D-732795 - sent 1/10/73  
15-73

## ABSTRACT

This report consists of an introduction in which journal reference is given for a major study concerned with the velocity distribution of the Scandinavian shield. In this published study, the errors of observation for the dispersion data were propagated into uncertainty estimates for the inverted crustal models for the first time. Refraction measurements of P and S velocities were used as a constraint during the inversion. The resulting models for Scandinavia give some indication of velocity inversions at the base of the sialic portion of the crust, at the base of the crust, and in the uppermost few tens of kilometers of the mantle. This study is made available in the main body of the present report. Additional recent research related to the Norwegian seismic array is also described.

Scientists contributing to the research under this contract: M. Landisman, Z. A. Der, F. Abramovici, and H. K. Gupta.

Unclassified

Security Classification

## DOCUMENT CONTROL DATA - R &amp; D

(Security classification of title, body of abstract and indexing annotation must be entered when the overall report is classified)

1. ORIGINATING ACTIVITY (Corporate author) The University of Texas at Dallas P.O. Box 30365 Dallas, Texas 75230		2a. REPORT SECURITY CLASSIFICATION Unclassified	
		2b. GROUP	
3. REPORT TITLE RESEARCH FOR DETERMINING PROPAGATION CHARACTERISTICS OVER ARPA'S NORWEGIAN ARRAY			
4. DESCRIPTIVE NOTES (Type of report and inclusive dates) Scientific Final 15 January 1970 - 28 February 1973		Approved 15 March 1973	
5. AUTHOR(S) (First name, middle initial, last name) Mark Landisman			
6. REPORT DATE February 1973	7a. TOTAL NO. OF PAGES 50	7b. NO. OF REFS 47	
8a. CONTRACT OR GRANT NO. F19628-70-C-0176	9a. ORIGINATOR'S REPORT NUMBER(S) Final Report (Part II)		
b. PROJECT NO., Task, Work Unit Nos. 5130 n/a n/a			
c. DoD Element 62701D	9b. OTHER REPORT NO(S) (Any other numbers that may be assigned this report) AFCRL-TR-73-0129		
d. DoD Subelement n/a			
10. DISTRIBUTION STATEMENT A - Approved for public release; distribution unlimited.			
11. SUPPLEMENTARY NOTES This research was supported by the Advanced Research Projects Agency.		12. SPONSORING MILITARY ACTIVITY Air Force Cambridge Research Laboratories (LW) L.G. Hanscom Field, Bedford, Mass.	
13. ABSTRACT		01730	
<p>This report consists of an introduction in which journal reference is given for a major study concerned with the velocity distribution of the Scandinavian shield. In this published study, the errors of observation for the dispersion data were propagated into uncertainty estimates for the inverted crustal models for the first time. Refraction measurements of P and S velocities were used as a constraint during the inversion. The resulting models for Scandinavia give some indication of velocity inversions at the base of the sialic portion of the crust, at the base of the crust, and in the uppermost few tens of kilometers of the mantle. This study is made available in the main body of the present report. Additional recent research related to the Norwegian seismic array is also described.</p>			

DD FORM 1473

2

Unclassified

Security Classification

LINK A

LINK B

LINK C

NAME	ROLE
1. [Name]	[Role]
2. [Name]	[Role]
3. [Name]	[Role]
4. [Name]	[Role]
5. [Name]	[Role]
6. [Name]	[Role]
7. [Name]	[Role]
8. [Name]	[Role]
9. [Name]	[Role]
10. [Name]	[Role]
11. [Name]	[Role]
12. [Name]	[Role]
13. [Name]	[Role]
14. [Name]	[Role]
15. [Name]	[Role]
16. [Name]	[Role]
17. [Name]	[Role]
18. [Name]	[Role]
19. [Name]	[Role]
20. [Name]	[Role]
21. [Name]	[Role]
22. [Name]	[Role]
23. [Name]	[Role]
24. [Name]	[Role]
25. [Name]	[Role]
26. [Name]	[Role]
27. [Name]	[Role]
28. [Name]	[Role]
29. [Name]	[Role]
30. [Name]	[Role]
31. [Name]	[Role]
32. [Name]	[Role]
33. [Name]	[Role]
34. [Name]	[Role]
35. [Name]	[Role]
36. [Name]	[Role]
37. [Name]	[Role]
38. [Name]	[Role]
39. [Name]	[Role]
40. [Name]	[Role]
41. [Name]	[Role]
42. [Name]	[Role]
43. [Name]	[Role]
44. [Name]	[Role]
45. [Name]	[Role]
46. [Name]	[Role]
47. [Name]	[Role]
48. [Name]	[Role]
49. [Name]	[Role]
50. [Name]	[Role]
51. [Name]	[Role]
52. [Name]	[Role]
53. [Name]	[Role]
54. [Name]	[Role]
55. [Name]	[Role]
56. [Name]	[Role]
57. [Name]	[Role]
58. [Name]	[Role]
59. [Name]	[Role]
60. [Name]	[Role]
61. [Name]	[Role]
62. [Name]	[Role]
63. [Name]	[Role]
64. [Name]	[Role]
65. [Name]	[Role]
66. [Name]	[Role]
67. [Name]	[Role]
68. [Name]	[Role]
69. [Name]	[Role]
70. [Name]	[Role]
71. [Name]	[Role]
72. [Name]	[Role]
73. [Name]	[Role]
74. [Name]	[Role]
75. [Name]	[Role]
76. [Name]	[Role]
77. [Name]	[Role]
78. [Name]	[Role]
79. [Name]	[Role]
80. [Name]	[Role]
81. [Name]	[Role]
82. [Name]	[Role]
83. [Name]	[Role]
84. [Name]	[Role]
85. [Name]	[Role]
86. [Name]	[Role]
87. [Name]	[Role]
88. [Name]	[Role]
89. [Name]	[Role]
90. [Name]	[Role]
91. [Name]	[Role]
92. [Name]	[Role]
93. [Name]	[Role]
94. [Name]	[Role]
95. [Name]	[Role]
96. [Name]	[Role]
97. [Name]	[Role]
98. [Name]	[Role]
99. [Name]	[Role]
100. [Name]	[Role]

WT

[illegible]

WT

[illegible]

WT

## Errors and resolution

## INTRODUCTION

A major investigation, based upon available data for the Scandinavian shield, was undertaken because of the impossibility of obtaining data from the Norwegian seismic array during most of the time during which this contract was valid. The inception of long period data acquisition on a moderately regular basis, which began only in the past several months, permitted us to scan the recent epicenter lists for those events deemed likely to generate higher mode surface wave trains travelling in favorable azimuths. These higher modes are essential if any useful resolution is to be achieved, as is demonstrated in the paper referenced below. A list of possible events was submitted to the Seismic Array Data Center in Alexandria, Virginia, and we are presently awaiting the transcription of digital data, plus phase calibration information. Requests for data from the same events and for phase calibration information have also been sent to the Research Institute of the Swedish National Defense (F.O.A.), in order to obtain corresponding digital recordings from long period instruments in the Hagfors array which is located not too far away, across the border in Sweden. An effort was begun late in the contract period to attempt the study of later passages of surface wave trains across the array, for more favorable events. These additional data may permit us to have an independent check on the accuracy of phase calibration information, as well as to increase the number of suitable wavetrains available for analysis. The late arriving data may also permit us to check on the separation of multimodal dispersion data. The effort required to pursue this approach, including tests for the suitability of events, proved to be time consuming, and the work carried over well into January 1973.

It is expected that the use of the augmented array aperture permitted by the joint analysis of digital data from the Norwegian and Swedish long period arrays may afford a means of

circumventing some of the problems to be expected from phase velocity studies of the Norwegian data alone. These problems are partially instrumental, involving uncertainties in phase response which will become less crucial as the aperture is expanded. Geological problems associated with the presence of the Oslo graben may also be ameliorated by separately studying its east flank with appropriate stations from both arrays. Additional studies within the Norwegian array may be able to help delineate the effects of local geology.

Problems of lateral refraction of wave trains, e.g. at continental margins, can now be largely circumvented through the use of homomorphic deconvolution and high resolution frequency wavenumber analysis. Both of these processes will be tried in order to accurately measure multimode data from the events selected.

It is expected that future studies such as those here described should contribute to more accurate knowledge of the seismic velocities beneath the Norwegian array. It should also help to refine the associated propagation delays, in order to assure more efficient operation of the array for purposes of detection.

#### PUBLICATION REFERENCE

Der, Z. A., and M. Landisman, "Theory for Errors, Resolution, and Separation of Unknown Variables in Inverse Problems, with Application to the Mantle and Crust in Southern Africa and Scandinavia", Geophys. J. R. astr. Soc., 27, pp. 137-178, 1972.

# **Theory for Errors, Resolution, and Separation of Unknown Variables in Inverse Problems, with Application to the Mantle and the Crust in Southern Africa and Scandinavia**

**Zoltan A. Der and M. Landisman**

(Received 1971 October 27)\*

## *Summary*

The geophysical inverse problem, the determination of the properties of the subsurface from a limited set of measurements, is basically non-unique. Separation of the unknown variables, the depth resolution, and the accuracy of the parameter estimates are three competing objectives which are reciprocally related.

The investigation of a set of free oscillation measurements having errors based upon those given by Derr revealed that the addition of overtones with low radial order numbers to the set of fundamental mode observations does not greatly improve the shear velocity depth resolution but does facilitate the separation of shear velocity from density.

Two sets of multi-mode surface wave dispersion measurements were inverted: the surface wave observations for Southern Africa reported by Bloch, Hales & Landisman, and a set of data for central Scandinavia as reported by Noponen, Porkka, Pirhonen and Luosto, and Crampin. Several models were obtained for each data set by varying the constraints used in the inversion process. The errors of the dispersion measurements were propagated into estimates of the accuracy of the inverted crustal models for the first time. Inclusion of shear and compressional velocity refraction measurements as a constraint on the inversion process leads to models for Scandinavia having some indication of velocity inversions at the base of the sialic portion of the crust, at the base of the crust, and in the first few tens of kilometres of the uppermost mantle.

## **1. Introduction**

This paper represents part of a continuing effort to improve current understanding of the physical properties of the crust and upper mantle using improved methods of data analysis and interpretation and a unified approach which considers diverse types of geophysical and geological information. The present study makes a number of contributions to the theory of the geophysical inverse problem, especially those areas concerned with the errors of measurement. It treats the effects of such errors on the depth resolution attainable for each variable of interest and the possible degree of separation of this variable from the others which also can influence the observations.

The geophysical inverse problem, which is an attempt to determine the Earth's physical properties from measurements of a set of gross earth data, has occupied the attention of a number of workers in recent years. In studies of particular importance

\*Received in original form 1971 June 23.

to the present approach Backus & Gilbert (1967, 1968) and Gilbert & Backus (1968) investigated the resolution obtainable from a set of *error-free* observations in terms of kernel functions which were constructed by linearly combining a set of partial derivatives corresponding to a given set of observations.

The effects of the measurement errors were recently presented by the present authors (Der, Massé & Landisman 1970, which will be referred to as Paper I), and independently in a major report by Backus & Gilbert (1970) using quite similar techniques. Important contributions to this subject may be found in two recent studies by Backus (1970a, b). The facts that the variances of the linear combinations of measurements are quadratic functions of the scalar coefficients, and that conveniently, the spread of the kernel functions can also be expressed as a quadratic function of these coefficients, are central to the methods adopted for evaluating the effects of measurement errors. The resulting optimization problem can be expressed in a form which is similar to that of classical least squares problems and the optimization problem is then solved easily with a computer. A trade-off curve between the spread of the kernel function and the associated error can be obtained by assigning relative weights to terms in the sum which is to be optimized.

An obvious extension of this work is the generalization to several unknown variables since several unknowns are involved in most actual inverse problems. Backus (1970c) treated several theoretical aspects of the problem of the separation of unknown variables but the cited work does not present numerical results as will appear in the material in Section 3 of this paper. Body wave velocities and density are usually sought in studies of the crust and upper mantle using observations of surface wave dispersion and free oscillations. The spatial distribution of the attenuation coefficients for the body waves is an additional objective if measurements of anelastic effects are included in the data.

It is desirable to separate the effects of all possible unknowns and at the same time to retain good resolution as a function of depth while retaining a reasonable variance for the estimators of each of the unknown parameters. The following discussion will illustrate the fundamentally competitive nature of these three objectives; any one of which may be satisfied only at the expense of the other two. The single parameter method can be used only if the rest of the parameters are known to sufficient accuracy. It is often assumed that all but one of the unknowns may be ignored when one parameter is predominant in influencing the measured data as is the case for shear velocity in surface wave measurements. The limitation of the problem to a study of only one variable may well be valid, if in the initial model the 'auxiliary' unknowns have been assigned values that are indeed correct. If the assigned values are inappropriate, however, the linear combination used to estimate the desired unknowns can depend considerably upon the inaccuracy of the selected values; it will also be modified by the contamination of the partial derivatives for the desired variable because of their sensitivity to the 'auxiliary' unknowns. As a consequence, the resulting solution will not be correct.

Some applications of the above theory will be presented in the following sections. The first concerns the resolution, errors of estimation, and separation of the shear velocity from the density in the mantle, using several sets of observations of the normal modes of free oscillation. The second example treats surface waves at intermediate distances, as they affect the problems of resolution, accuracy, and separation of variables for the crust. In addition, surface wave observations for Southern Africa, and dispersion and refraction data for Scandinavia use insights derived from the present theory as constraints in an inversion process which yields the vertical distribution of physical parameters for the crust and upper mantle in these two shield areas. The errors of the dispersion measurements are propagated into errors of the inverted crustal models, and the significance of various features are discussed in terms of these errors.

## 2. Theory

The following derivation of the relation between resolution and separation of two unknown variables is an obvious extension of the theory in Paper I, and although developed independently, is related to the discussion on resolution presented by Backus & Gilbert (1970) and Backus (1970a, b), and to the discussion on separation of variables given by Backus (1970c). The main points will be repeated here, however, to make the present paper self-contained.

The development begins with an initial model consisting of  $M$  homogeneous layers. The parameter of interest  $p_k$  in layer  $k$  will be estimated by a linear combination  $A_k$  of the  $N$  observations  $C_i$ , which are defined as the differences between the observed quantities and those corresponding to the initial model. It is assumed that the quantities  $C_i$  and  $A_k$  are small enough to insure that linear theory applies in the first approximation.

The linear combination used as the estimator of the desired parameter

$$A_k = \sum_{i=1}^N \alpha_{ik} C_i \quad (1)$$

is normalized such that

$$\epsilon_{kk} = \sum_{i=1}^N \alpha_{ik} P_{ik} = 1, \quad (2)$$

which implies that a unit change of the desired parameter  $p_k$  in the layer  $k$  corresponds to a unit change of  $A_k$ . In (2), the partial derivatives are written

$$P_{ik} = \frac{\partial C_i}{\partial p_k}. \quad (3)$$

The first of the three objectives of the problem is the minimization of the variance of the linear combination

$$\text{var } A_k = \sum_{i=1}^N \sum_{j=1}^N \alpha_{ik} \alpha_{jk} \text{cov}(C_i, C_j), \quad (4)$$

which takes the form

$$\text{var } A_k = \sum_{i=1}^N \alpha_{ik}^2 \text{var } C_i \quad (5)$$

for independent observational errors.

The other two objectives require minimization of the quantities

$$s_1^2 = \sum_{j=1}^M W_j \epsilon_{jk} \quad j \neq k \quad (6)$$

and

$$s_2^2 = \sum_{j=1}^M W_j \bar{\epsilon}_{jk}, \quad (7)$$

where  $W_j$  are the layer thicknesses expressed in terms of a pre-selected standard thickness. (The standard layer thickness was set at 1 km for the mantle calculations and 4 km for the crustal calculations in this paper.) The minimizations in (6) and (7) increase the resolution for the desired parameters  $p$  and reduce the dependence on a second undesired set of parameters  $\bar{p}$ , respectively. The quantities  $s_1$  and  $s_2$ , which

have dimensions of  $(\text{km})^{\frac{1}{2}} \times$  (the applicable partial derivative), are used as relative indicators of the depth resolution and of the separation of sensitivity between the desired and undesired physical parameters. The quantities  $\varepsilon_{jk}$  and  $\bar{\varepsilon}_{jk}$  are defined

$$\varepsilon_{jk} = \sum_{i=1}^N \alpha_{ik} P_{ij} \quad j \neq k \quad (8)$$

$$\bar{\varepsilon}_{jk} = \sum_{i=1}^N \alpha_{ik} P_{ij}, \quad (9)$$

where  $P_{ij}$  is defined as in (3) and

$$P_{ij} = \frac{\partial C_i}{\partial \bar{p}_j}. \quad (10)$$

To achieve these minimizations and thus determine the coefficients  $\alpha_{ik}$ , the sum

$$E = \sin \beta \text{ var } A_k + \cos \beta \cos \eta s_1^2 + \cos \beta \sin \eta s_2^2 \quad (11)$$

must be minimized subject to the condition (2).  $\beta$  and  $\eta$  are adjustable parameters which determine which one of the three minimizations is to be the most effective.

Obviously this minimization has physical meaning only if

$$0 \leq \beta \leq \frac{1}{2}\pi$$

$$0 \leq \eta \leq \frac{1}{2}\pi.$$

The extreme values of  $\beta$  and  $\eta$  give cases where at least one of the minimizations is disregarded.

The function

$$\sigma_A = F(s_1, s_2) \quad (12)$$

gives a *trade-off surface* in the space defined by (a) the standard deviation  $\sigma_A = \sqrt{(\text{var } A_k)}$  of the linear combination for the desired parameters, (b) the resolution of these parameters  $p$ , and (c) the separation of the parameters  $p$  from the undesired parameters  $\bar{p}$ .

The minimization problem can be solved with the help of the Lagrange multiplier  $\mu$ , yielding

$\sin \beta V$ $+ \cos \beta \cos \eta \Gamma$ $+ \cos \beta \sin \eta \Gamma$	$P_{1k}$ $P_{2k}$ $\vdots$ $\vdots$ $P_{Nk}$	$\alpha_{1k}$ $\alpha_{2k}$ $\vdots$ $\vdots$ $\alpha_{Nk}$	$=$	$0$ $0$ $\vdots$ $\vdots$ $0$	(13)
$P_{1k} P_{2k} \dots \textcircled{P_{Nk}} \longrightarrow \longrightarrow \longrightarrow \longrightarrow$	$0$	$\mu$	$1$		

where  $V$ ,  $\Gamma$ , and  $\bar{\Gamma}$  are  $N \times N$  square matrices having elements

$$\left. \begin{aligned} V_{in} &= \text{cov}(C_i, C_n) \\ \Gamma_{in} &= \sum_{j=1}^M W_j P_{ij} P_{nj} \quad j \neq k \\ \bar{\Gamma}_{in} &= \sum_{j=1}^M W_j \bar{P}_{ij} \bar{P}_{nj} \end{aligned} \right\} \quad (14)$$

The matrix  $V$  is assumed to be diagonal in the subsequent calculations. This assumption implies that the data have been properly selected to insure that the errors of measurement are independent.

Various parts of the trade-off surface can be investigated by changing the parameters  $\beta$  and  $\eta$ .  $\sigma_A$  can be improved at the expense of increases in  $s_1$  and  $s_2$ . This process is equivalent to increasing the peak widths and side lobes of the approximate delta functions formed by calculation of the linear combinations of partial derivatives. If  $\sigma_A$  is kept constant, a trade-off curve can be obtained between  $s_1$  and  $s_2$ , showing the relation between the resolution in the desired variable and the dependence on the undesirable variable. In general, if the chief objective is a linear combination which depends very little on other unknowns, the resolution in the desired variable must be sacrificed.

The interrelationship of the quantities  $s_1$ ,  $s_2$ , and  $\sigma_A$  demonstrates the basic non-uniqueness of the inverse problem. There are an infinite number of solutions to any inverse problem. The observations  $C_i$ , which are the differences between the observed quantities and those which can be derived from the initial model, can be explained by an infinite number of parameter distributions. For instance, if high vertical resolution is assumed ( $\sigma_A$  is small), the resulting model will have large fluctuations of a single parameter in adjacent layers ( $s_2$  is large). An alternate solution can be constructed by permitting several parameters to change with relatively longer vertical wave-lengths.

There is no 'best' solution based on the given set of data  $C_i$  above. Very often however, other information is available which restricts the available range of models. One obvious restriction is linearity. It is assumed in the present algorithm that the observations depend linearly upon the parameters of the models. Linearity no longer applies, however, if the differences between the initial model and final solution exceed a certain limit. The range of solutions for seismic measurements is further restricted by other limitations, such as those produced by petrological, gravitational, and tectonic considerations.

The simplicity of the algorithm shown above makes it suitable for rapid calculations on a digital computer. Naturally, other measures of spread could be used, or limits could be placed on the ranges of the unknown coefficients, but these measures would result in increasing the complexity of the calculations. It seems, therefore that most of the desired information can be conveniently obtained using this simple method.

### 3. Determination of density and shear velocity in the mantle when the observational errors are specified

The inverse problem for the mantle has been the subject of numerous investigations. The present discussion will be restricted to the question of the simultaneous determination of the shear velocity and density in the mantle; more detailed accounts of the development of the inverse problem may be found in reviews such as those by Press (1966), Anderson (1967), and Derr (1969).

Dziewonski (1970) investigated the resolution obtainable from various sets of free oscillation data and pointed out that the strong correlation between the partial derivatives with respect to density and shear velocity makes the process of inversion highly non-unique in certain regions within the Earth. Backus (1970c) has presented an elegant discussion of the conditions required for the separation of multiple variables from a finite set of inaccurate gross earth data.

This section will present a brief analysis of the problem of resolution of variables in the presence of measurement errors. The partial derivatives used in this section are those published by Wiggins (1968). These derivatives were computed for parameter changes at layer interfaces, after assuming that density changes linearly and the body wave velocities follow a power law between neighbouring interfaces. The published derivatives were approximately converted to derivatives with respect to parameter changes corresponding to layers of unit thickness centred at the published interfaces since the original functions were not quite suitable for the present calculations. The converted derivatives were appropriately weighted for subsequent calculations in order to take into account the variations in distance between interfaces.

The data selected for analysis include 26 fundamental mode free oscillations divided evenly between spheroidal and torsional modes. In addition, a set of higher mode observations is also included. The higher modes chosen have been repeatedly observed and are therefore considered to be reliable.

The amount of data used may seem to be very limited, but it must be kept in mind that the partial derivatives of modes with nearly equal colatitudinal order numbers are usually highly dependent upon each other, and therefore, furnish no additional information, especially at higher order numbers. The modes to be used were selected for orders  $n$  which are approximately related by the factor  $\sqrt{2}$ . This procedure was followed only approximately since the set of partial derivatives published by Wiggins (1968) was incomplete.

Table 1 shows the standard deviations of the mean (in seconds) for commonly observed modes of free oscillation of the Earth. The values for the lower colatitudinal order numbers were taken from estimates for the standard deviations of the mean, for observations through the year 1968 (Derr 1969). Other values in the table differ

Table 1

*Estimated measurement errors (s) for observations of free oscillations*

Mode	Standard error of the mean	Mode	Standard error of the mean	
${}_0S_2$	2.0	${}_0T_2$	10.00	
${}_0S_3$	0.6	${}_0T_3$	2.40	
${}_0S_4$	0.7	${}_0T_4$	1.29	${}_cT_4$
${}_0S_6$	0.7	${}_0T_6$	0.70	
${}_0S_8$	0.2	${}_0T_8$	0.40	
${}_0S_{12}$	0.12	${}_0T_{12}$	0.29	
${}_0S_{16}$	0.12	${}_0T_{17}$	0.25	
${}_0S_{24}$	0.11	${}_0T_{21}$	0.25	
${}_0S_{37}$	0.16	${}_0T_{33}$	0.32	
${}_0S_{48}$	0.14	${}_0T_{40}$	0.35	
${}_0S_{61}$	0.12	${}_0T_{57}$	0.20	
${}_0S_{67}$	0.13	${}_0T_{74}$	0.15	
${}_0S_{97}$	0.12	${}_0T_{93}$	0.13	
${}_1S_2$	1.30	${}_1T_4$	0.75	
${}_1S_4$	0.85	${}_1T_6$	0.7	
${}_1S_6$	0.42	${}_1T_9$	0.6	
${}_1S_8$	0.80	${}_1T_{12}$	0.5	
${}_2S_3$	0.60	${}_1T_{14}$	0.4	
${}_2S_6$	0.59	${}_1T_{16}$	0.4	
${}_2S_{14}$	0.30			

slightly from published estimates, as discussed below. The standard deviations were set at 0.05 per cent of the free oscillation period in cases for which no estimates were available. The standard deviations were increased for periods less than 170 s, since the effects of lateral inhomogeneities in the upper mantle decrease the reliability of these observations and cause them to be observed less frequently. The standard deviations given for some of the modes, especially the moderately higher orders, may seem to be excessively low. It must be remembered, however, that observations of free oscillations are not independent. If a free oscillation period deviates from that computed for a starting model, the free oscillations with nearly equal colatitudinal order numbers will also tend to deviate in the same sense. Therefore, the errors can be decreased by approximately 30 per cent compared to the error for an individual observation, by taking averages of the observations for several neighbouring free oscillation periods. The standard deviation given by Derr (1969a) for  ${}_0S_2$  is about 0.49, but since there are doubts about the identification of this mode, the standard deviation was set equal to 2. One of the modes in Table 1 is  ${}_2S_{14}$ , which has not been observed. It takes the place of the group  ${}_2S_{10}$ ,  ${}_2S_{15}$ , and  ${}_2S_{16}$ , which have been observed, but for which no partial derivatives were available in the tables presented by Wiggins (1968). This substitution is of no great consequence since the partial derivatives in this range are all very similar.

Backus & Gilbert (1970) have shown that the standard errors of all linear combinations of a set of observations increase by the factor  $N$  if the standard errors of each of the observations are increased by this same factor. Therefore, if future evidence should indicate that the error estimates of the observations ought to be multiplied by some factor  $N$ , this same factor may also be applied to the standard errors of the linear combinations, if the same factor is uniformly applied to all members of the data set.

Figs 1-4 show the trade-off curves for error, resolution, and separation of variables. The shear velocity is taken to be the desired variable throughout this section and the density is considered to be the variable to be eliminated. The vertical axis corresponds to the standard deviation,  $\sigma_A$ , of the linear combination used to obtain the estimator  $A_k$ , while the quantities characteristic of the resolution and separation of variables,  $s_1$  and  $s_2$ , are plotted on the horizontal axis as thick and thin lines, respectively.

Four modal combinations were used: the set of fundamental mode spheroidal observations (denoted by  ${}_0S_n$  in Figs 1-4), the sum of the selected fundamental spheroidal and torsional modes ( ${}_0S_n + {}_0T_n$ ), the set including all of the fundamental modes and the higher torsional modes ( ${}_0S_n + {}_0T_n + {}_1T_n$ ) and the sum of all modes given in Table 1 ( ${}_0S_n + {}_0T_n + {}_1T_n + {}_1S_n$ ).

The uppermost parts of the curves represent the condition  $\beta = 0$  in equation (11). This value of  $\beta$  implies that only the resolution and/or the separation of parameters is optimized, without regard to the variance of the corresponding linear combinations. When  $\beta = 0$ , the errors of observation are ignored; the resolution and mode separation are determined solely by the shapes of partial derivative curves as functions of depth, and by the intercorrelations between the partial derivatives with respect to the two variables, shear velocity and density. This case has been investigated exhaustively by Dziewonski (1970).

The lowest parts of the curves correspond to the case  $\beta = 90^\circ$ . The coefficients of the linear combinations for this case are determined solely by the relative errors assigned to the measurements and by the normalization conditions. Thus the curves corresponding to various values of  $\eta$  all converge to one point at the lowest points of these curves.

Three values of the weighting parameter  $\eta$  were used;  $0^\circ$ ,  $45^\circ$  and  $90^\circ$ . The value  $\eta = 0^\circ$  optimizes the resolution without regard to separation of the desired parameter from the undesirable one.  $\eta = 90^\circ$ , on the other hand, only optimizes the separation

Depth 146 km

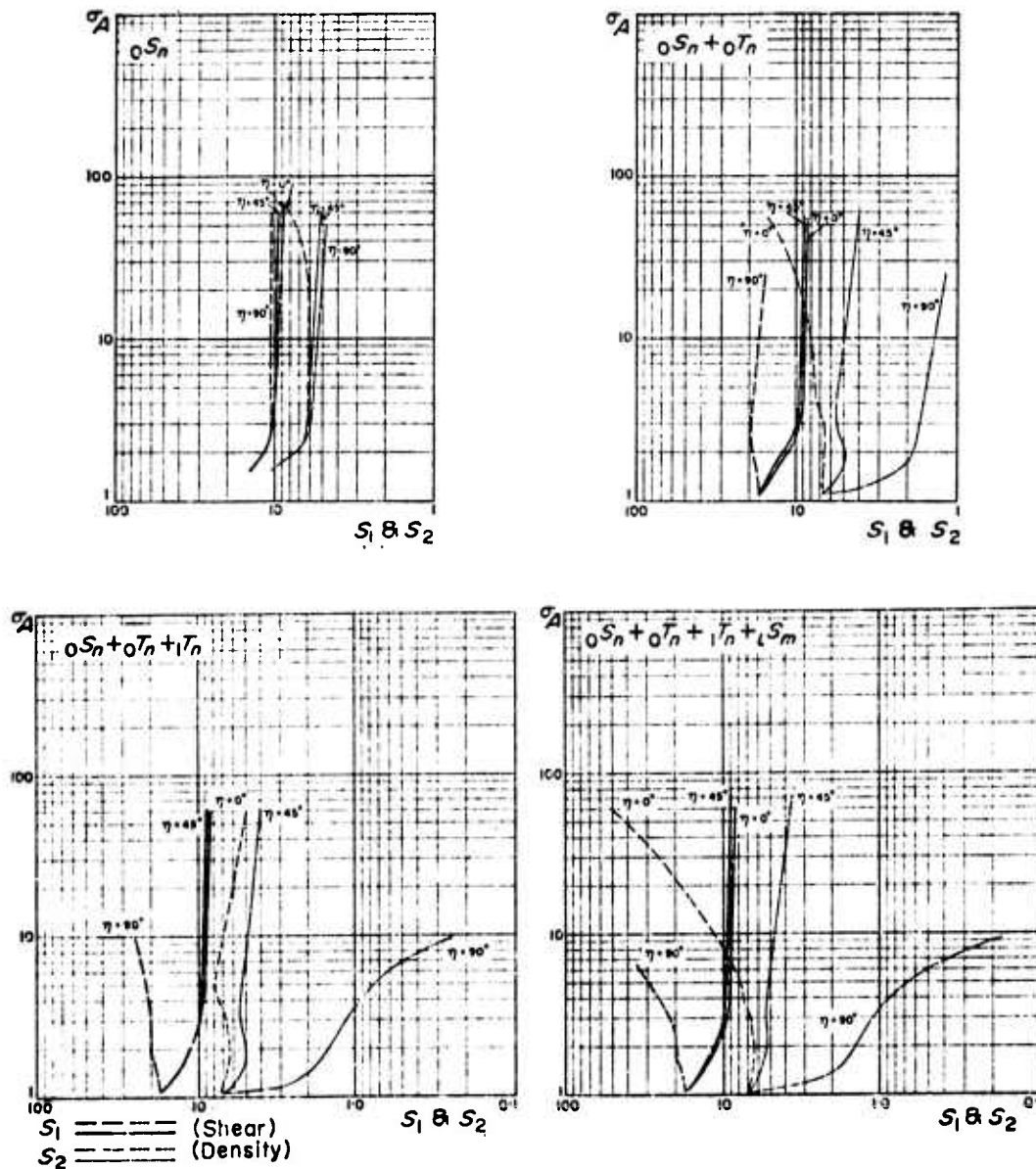


FIG. 1. Trade-off curves for various combinations of normal mode observations. The achievable standard deviation  $\sigma_A$ ,  $\text{km s}^{-1}$  for shear velocity and  $\text{g cm}^{-3}$  for density, for a linear combination of observations having errors given in Table 1, is shown as a function of  $s_1$ , the depth resolution indicator, and  $s_2$ , the indicator which measures the discrimination between the physical parameters of density and shear velocity. Shear velocity (heavy lines) is the desired variable, and density (light lines) is the variable to be suppressed. The value of the shear velocity is sought at a depth of 146 km.

of parameters, yielding a poor resolution in the desired variable. If  $\eta$  is set equal to an intermediate value such as  $45^\circ$ , both resolution and separation of variables may be optimized simultaneously. Such intermediate values of  $\eta$  have no absolute significance since the relative weighting of the terms in the optimization procedures, and therefore the relative degree of optimization, is a complicated function of the shapes and relative values of the partial derivatives for each depth range to be considered.

Thick curves in Figs 1-4 correspond to the shear velocity resolution parameter  $s_1$ , and thin lines to the parameter  $s_2$ , which is a measure of the separation of the two

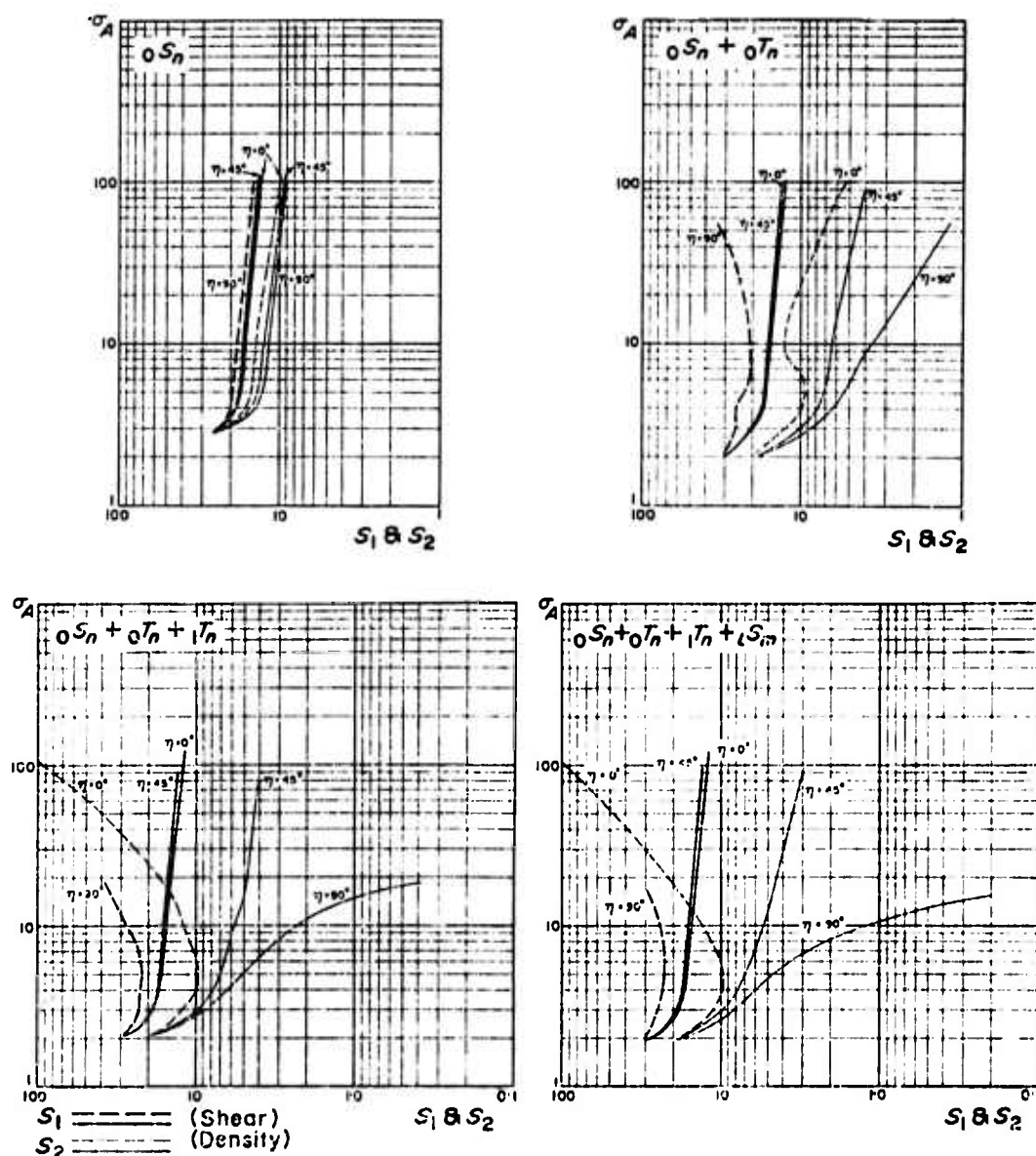


FIG. 2. Trade-off curves for shear velocity determination at a depth of 496 km.  
See caption, Fig. 1 for details.

variables. Dashed lines denote the curves  $s_2$  at  $\eta = 0^\circ$  and  $s_1$  at  $\eta = 90^\circ$ . These curves represent unconstrained solutions of equation (11), which change erratically and are somewhat uncertain. The figures show the trade-off curves at four different depths: 146, 496, 1071 and 2821 km.

Inspection of the trade-off curves shows that the curves for  $s_1$  change little with the inclusion of modes in addition to the fundamental spheroidal modes, for values of  $\eta$  between  $0^\circ$  and  $45^\circ$ . There is, however, considerable change in the  $s_2$  curves within this range. Inspection of the corresponding delta function approximations shows some improvement in the shape of these approximate delta functions, but the main improvement as  $\eta$  increases comes from the increased effectiveness for the separation of parameters, as evidenced by the decreasing values for  $s_2$  (thin curves).  $\eta = 90^\circ$  is associated with the best possible separation of parameters, (furthest right thin curve in all of these figures) but the corresponding resolution in shear velocity (heavy broken

Depth 1071 km

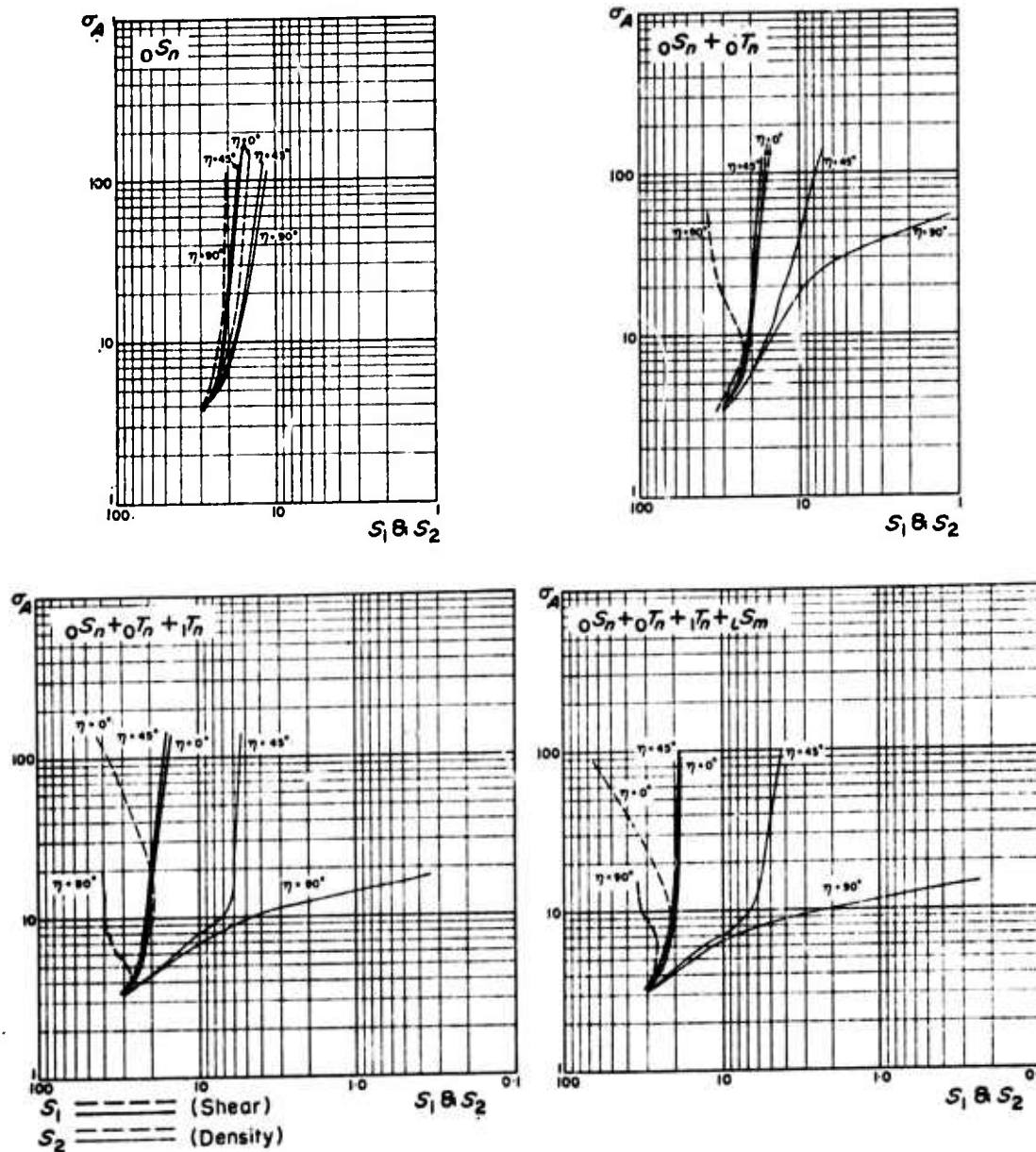


FIG. 3. Trade-off curves for shear velocity determination at a depth of 1071 km.  
See caption, Fig. 1 for details.

lines at left) is unacceptably poor. Therefore the most useful linear combinations are those in the vicinity of  $\eta = 45^\circ$ , where both the separation of variables and the resolution in shear velocity are acceptable.

The thick trade-off curves for the shear velocity resolution,  $s_1$ , associated with values  $0^\circ < \eta < 45^\circ$  are quite steep. This steepness implies that the standard deviation  $\sigma_k$  of the linear combination  $A_k^H$ , which is the estimator of the shear velocity, can be considerably improved with a relatively small decrease in shear velocity resolution. The 'optimum point' thus lies close to the lower right 'corner' of the heavy curves of shear velocity resolution, for values of  $\eta$  in the range  $0^\circ$ – $45^\circ$ , where a moderate degree of separation between shear velocity and density is possible. There appears to be some decrease in the effectiveness of the separation of variables in this range, since some of the curves for  $s_1$  and  $s_2$  converge near  $\beta = 90^\circ$ .

The absolute values of coefficients of the various linear combinations reveal the

Depth 2821 km

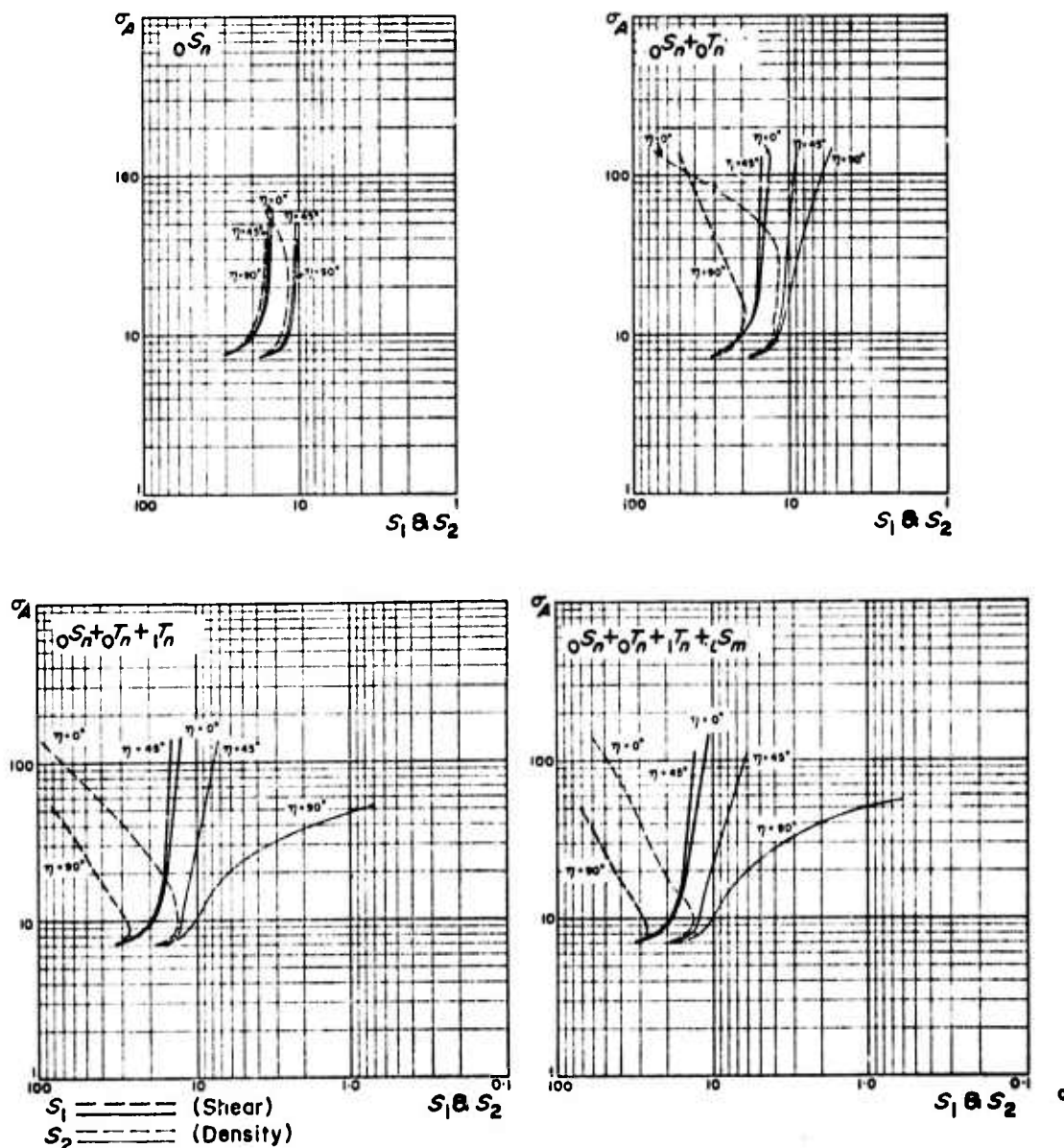


FIG. 4. Trade-off curves for shear velocity determination at a depth of 2821 km. See caption, Fig. 1 for details.

relative importance of various observations in determining and resolving the shear velocities within the mantle. The largest weights are associated with the fundamental spheroidal modes for  $0^\circ < \eta < 45^\circ$ .

Spheroidal mode observations of high co-latitudinal order numbers predominate if only the fundamental modes are used at shallow depths, although occasional higher order torsional modes must also be considered. Low-order spheroidal modes must be given the greatest weights for the determination of shear velocity at greater depths.

Non-uniqueness in inverse problems results not only from the limited resolution with depth but from the inter-correlation of partial derivatives with respect to each of the unknown parameters. Dziewonski (1970) investigated this intercorrelation of the partial derivatives of the free oscillation periods with respect to shear velocity and density. It is now worthwhile to re-evaluate these results, taking proper account of the errors of measurement. Intercorrelation of the variables can be made evident by plotting the dependence of linear combinations of shear velocity and density, which

are expressed by the numbers  $\epsilon_{jk}$  and  $\bar{\epsilon}_{jk}$  respectively, as functions of depth. Fig. 5 shows plots for the data set consisting of the fundamental spheroidal and torsional modes. The positive intercorrelation between the partial derivatives for shear velocity and density is indicated by the peak in sensitivity to density (dashed curve) located at about the same depth as the peak of the approximate delta function for shear velocity. In addition, negative intercorrelations at various depths are also evident, especially those between shear velocity and density at a shallower depth, as noted by Dziewonski

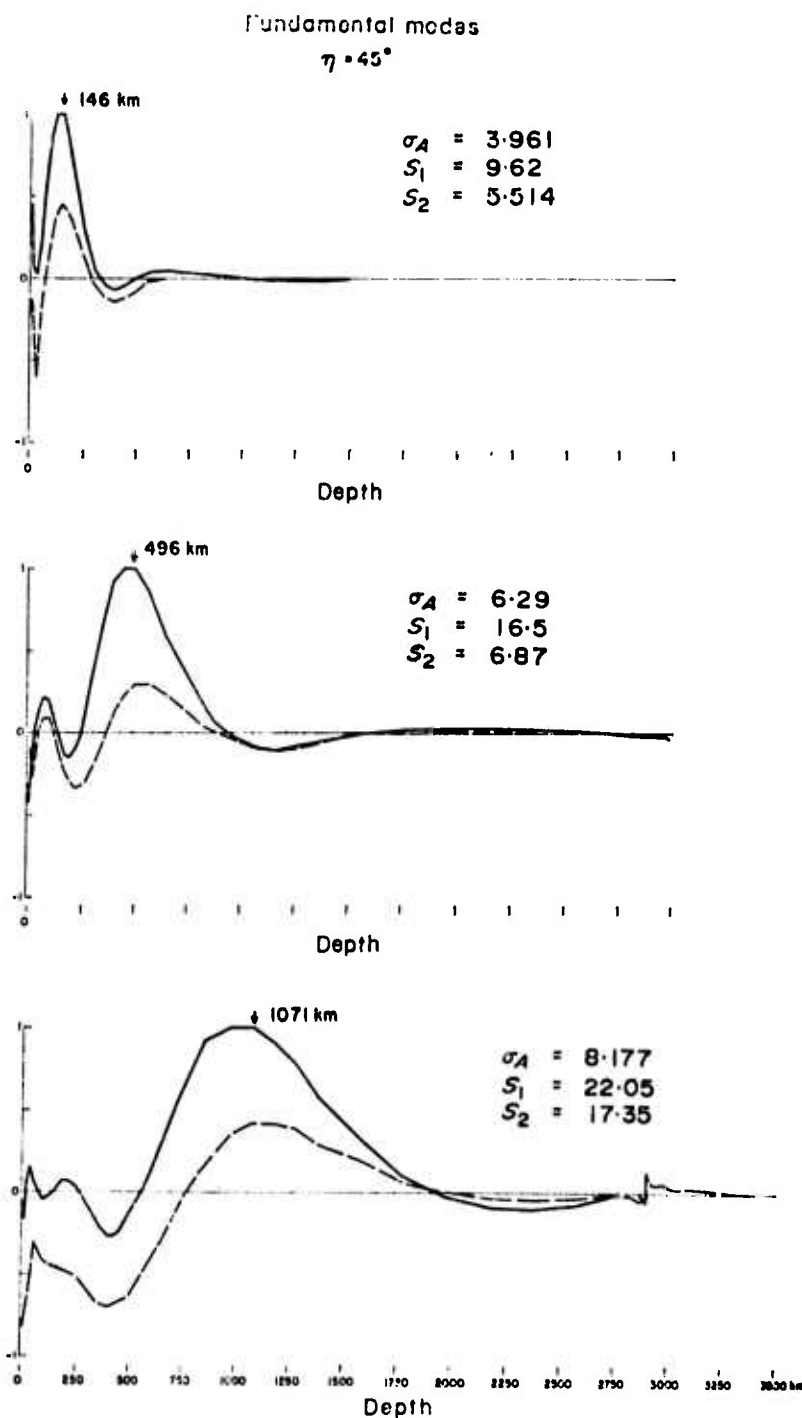


FIG. 5. Delta function approximations obtained for the mantle by using the *fundamental mode* free oscillations and associated errors for the data set given in Table 1. Solid lines give the approximate delta functions which show the sensitivity of these data to changes in shear velocity as a function of depth; dashed lines show the corresponding sensitivity to changes in density.

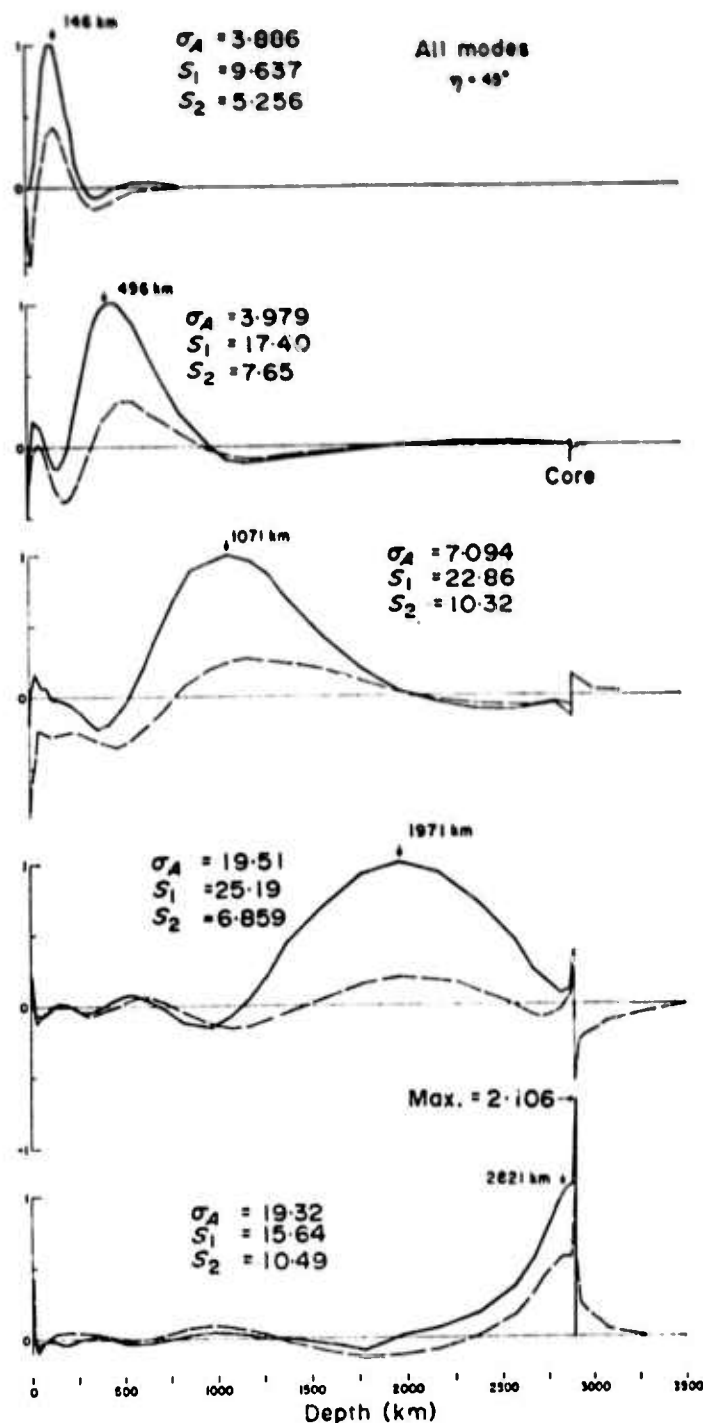


FIG. 6. Delta function approximations for the mantle obtained by using all the modes given in Table 1. See caption, Fig. 5.

(1970). The set of partial derivatives used by Dziewonski had a greater number of modes with high co-latitudinal order numbers. Many of these modes were eliminated in the present study since most of the corresponding partial derivatives were interdependent. The same higher order derivatives are properly re-emphasized by the present procedure since these modes have relatively small observational errors.

Inspection of the plots of the approximate delta functions in Fig. 5 yields information about the accuracy, and thus the significance, of the velocity adjustments obtainable with a given vertical resolution, during the process of inversion. This information can be derived by dividing the standard error of the linear combination by the vertical

depth range of the peaks of the approximate delta functions. The vertical depth range can be defined as the width of the peak where the value of the approximate delta function is close to unity ( $\sim 0.8$ ). The approximate values of minimum detectability for changes in shear velocity may be estimated by assuming that these changes become detectable if they exceed the expected standard deviation of the linear combination  $\sigma_A$ , which is calculated for a unit layer thickness of 1 km for these studies of the mantle. The minimum detectable change in shear velocity is thus approximately  $0.04 \text{ km s}^{-1}$  spread over a 100-km range centred in the vicinity of depths near 150 km, about  $0.015 \text{ km s}^{-1}$  for a 250-km range at depths near 500 km, and  $0.015\text{--}0.02 \text{ km s}^{-1}$  for a 500-km range at depths of about 1000 km, if only fundamental mode observations are considered.

Fig. 6 shows similar plots for the total combination of modes. The figures do not show much change relative to the plots for the fundamental modes at shallower depths. In the deeper part of the mantle the separation of the two variables becomes increasingly effective as more modes are added.

#### 4. Multi-mode crustal surface wave dispersion observed at intermediate distances

##### *Partial derivatives for the crust in a shield area*

The resolution and separation of variables for multimode surface wave observations at intermediate distances also can be treated with the foregoing theoretical techniques. The initial shield model is identical to the one previously used for partial derivatives by Bloch, Hales & Landisman (1969), and by the present authors in Paper I. Partial derivatives of the phase and group velocities with respect to the layer compressional velocities and densities were computed in order to extend the previous investigation to several variables. The spherical approximations devised by Alterman, Jarosch & Pekeris (1961) and Bolt & Dorman (1961) were used for these calculations. The results for Love waves were checked subsequently against those obtained by the exact transformation presented by Biswas & Knopoff (1970), and Gerver & Khazdan (1968). Both sets of calculations were concordant in the period range of interest. Our Love wave program, which uses the matrix method of Haskell (1960), failed to give results during attempts to calculate dispersion for thick layer sequences at high frequencies. It was necessary to omit the lower portion of the layered model, which did not influence the dispersion, since the particle motion was zero at those depths, and to split the layers in order to bypass this difficulty. The Rayleigh wave program uses Dunkin's (1965) algorithm, which enables one to obtain greater numerical stability at higher frequencies, and did not pose any such problems. The application of the exact transformation seemed to contribute to the difficulties associated with the Love wave program. New approaches, such as that given by Schwab & Knopoff (1970), should eliminate many of these difficulties. The new partial derivatives calculated for this study are shown in Figs 7–12. Phase and group velocity dependence upon density are presented in Figs 9 and 10, while the effects of compressional velocity changes appear in Fig. 11. Fig. 12 shows the influence of changes in the depth of the Mohorovičić discontinuity. All partial derivatives were normalized with respect to a layer thickness of 4 km, and were plotted as functions of depth for various periods. Points were plotted at the mid-points of layers and connected by straight lines in an attempt to visually smooth the discrete nature of these derivatives.

Many aspects of the inversion problem can be directly noted by the inspection of these plots. They exhibit abrupt changes in slope at depths corresponding to prominent interfaces, such as the Conrad discontinuity (20-km depth), and the Mohorovičić discontinuity (40-km depth). The changes would be even more abrupt if the layer thicknesses were considered to be infinitesimal. These abrupt changes produce singular effects near the interfaces but do not affect the overall resolution very much. Many of the results presented in our previous study (Paper I) can also be easily

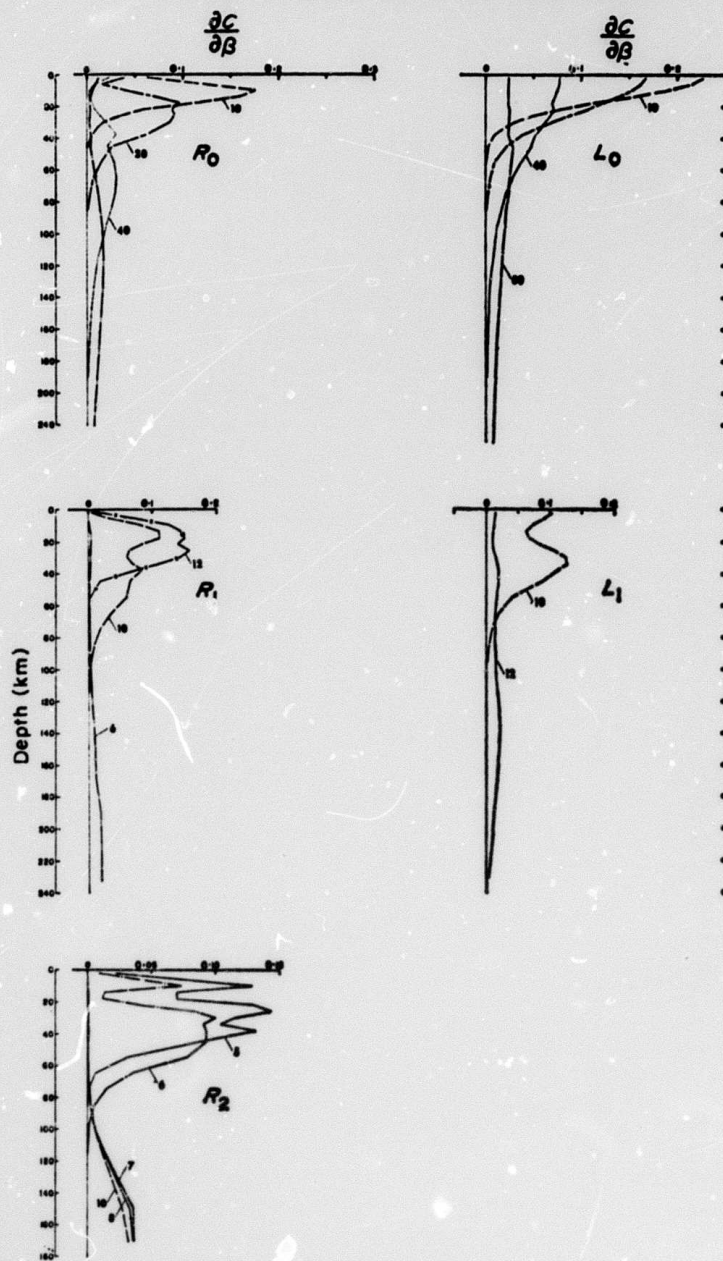


FIG. 7. Selected partial derivatives of phase velocities with respect to shear velocity for shield model. Normalized to 4-km layer thickness.

understood in terms of these curves. The relatively smaller peak values and smoother shapes of the fundamental Love wave partial derivative curves, as compared to the fundamental Rayleigh wave partial derivatives, explains why the resolution of fundamental Love wave measurements is inferior to that obtainable from the fundamental Rayleigh wave data. The drastically different shapes of the higher mode partial derivative curves facilitate the buildup of good delta function approximations; the improvement in resolution resulting from the inclusion of higher mode data is a direct consequence of these improved approximations.

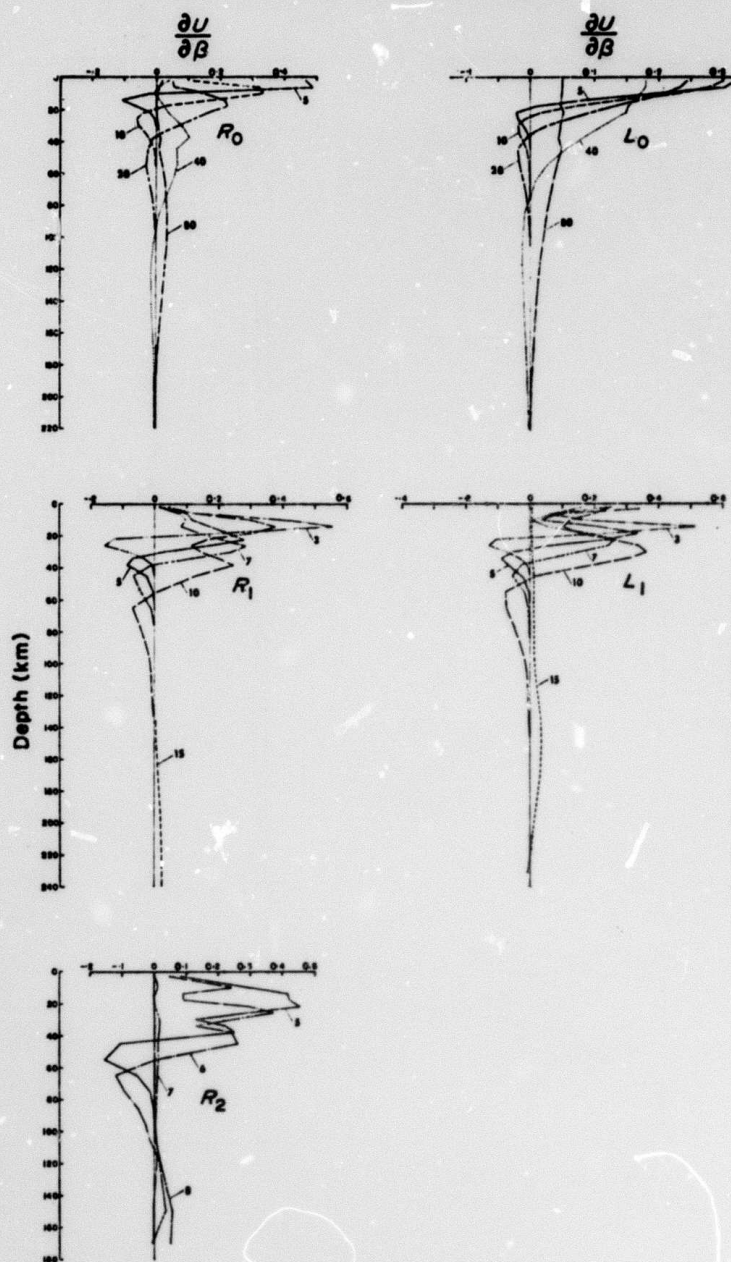


FIG. 8. Selected partial derivatives of group velocities with respect to shear velocity for shield model.

The partial derivatives with respect to compressional velocity and density are considerably smaller, although not negligible, compared to the partial derivatives with respect to shear velocity. This is often considered to be a justification for the use of surface wave measurements for the determination of shear velocity alone, without regard to the other variables. Changes of shear velocity alone, however, can produce media with petrologically unreasonable Poisson's ratios and densities. Poisson's ratio and density may be adequately controlled by using a linear combination of partial derivatives with respect to all of the variables in the inversion. The shear

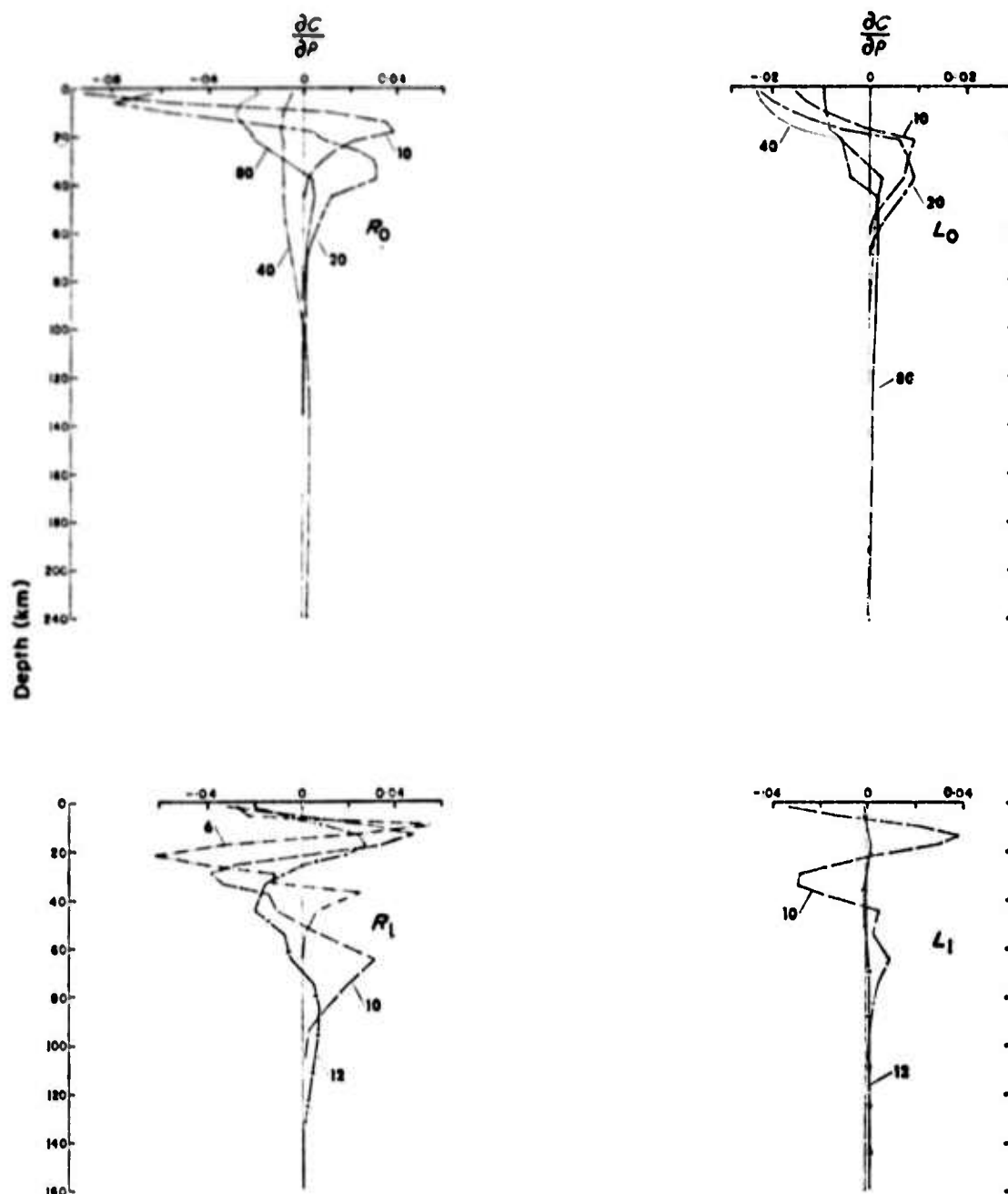


FIG. 9. Selected partial derivatives of phase velocities with respect to density for shield model.

velocity solution thus obtained will be modified, but only slightly, since the sensitivity of the surface waves to density and compressional velocity changes is relatively low.

The magnitudes of the partial derivatives of the phase velocities are smaller than those for the group velocities. Thus the resolution for observations of phase velocity is inferior to that for group velocity observations, if the errors are equal. Moreover, the partial derivatives of phase velocity have simpler shapes, which also may hinder the buildup of delta functions.

The following sections will treat the relative importance of the shear and compressional velocities, and of the density in determining the surface wave velocities. The data set and the errors are slightly modified relative to those used previously in Paper I; the new values are given in Table 2. The relative importance of two pairs of variables,

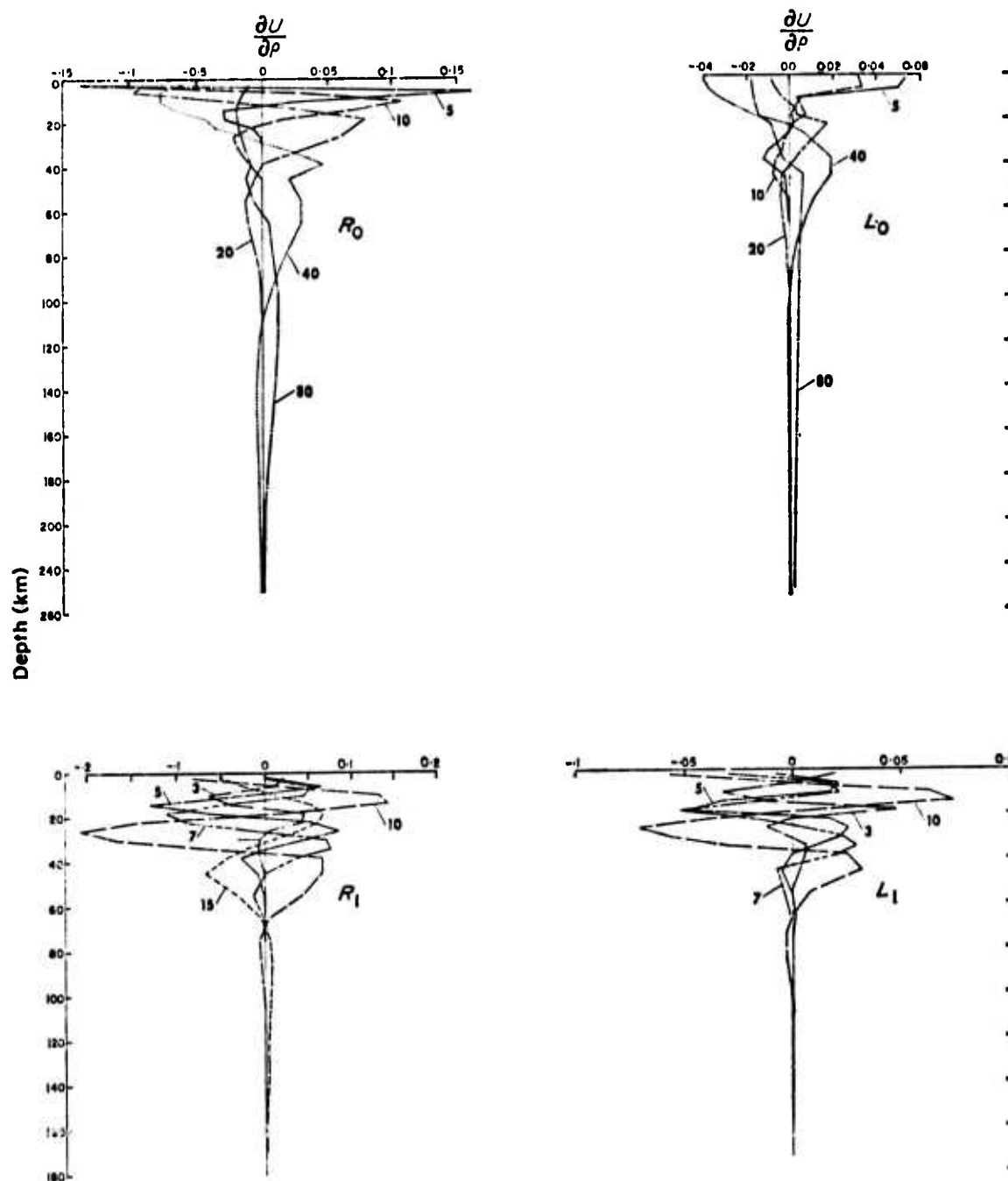


FIG. 10. Selected partial derivatives of group velocities with respect to density for shield model.

shear velocity vs. density, and shear velocity vs. compressional velocity, is determined by the shapes and absolute magnitude of the partial derivative curves.

#### *Shear velocity vs. density*

The partial derivatives of surface wave group velocities with respect to the density are, on the average, less than one half of the magnitude of the derivatives with respect to shear velocity, as shown in Figs 8 and 10. The derivatives are not negligible, however, and the effect of density changes should be taken into account.

Fig. 13 shows the delta function approximations for observations consisting of only fundamental mode data; corresponding results for the total data set are shown in Fig. 14. The case in which the shear velocity is the desired variable and the density

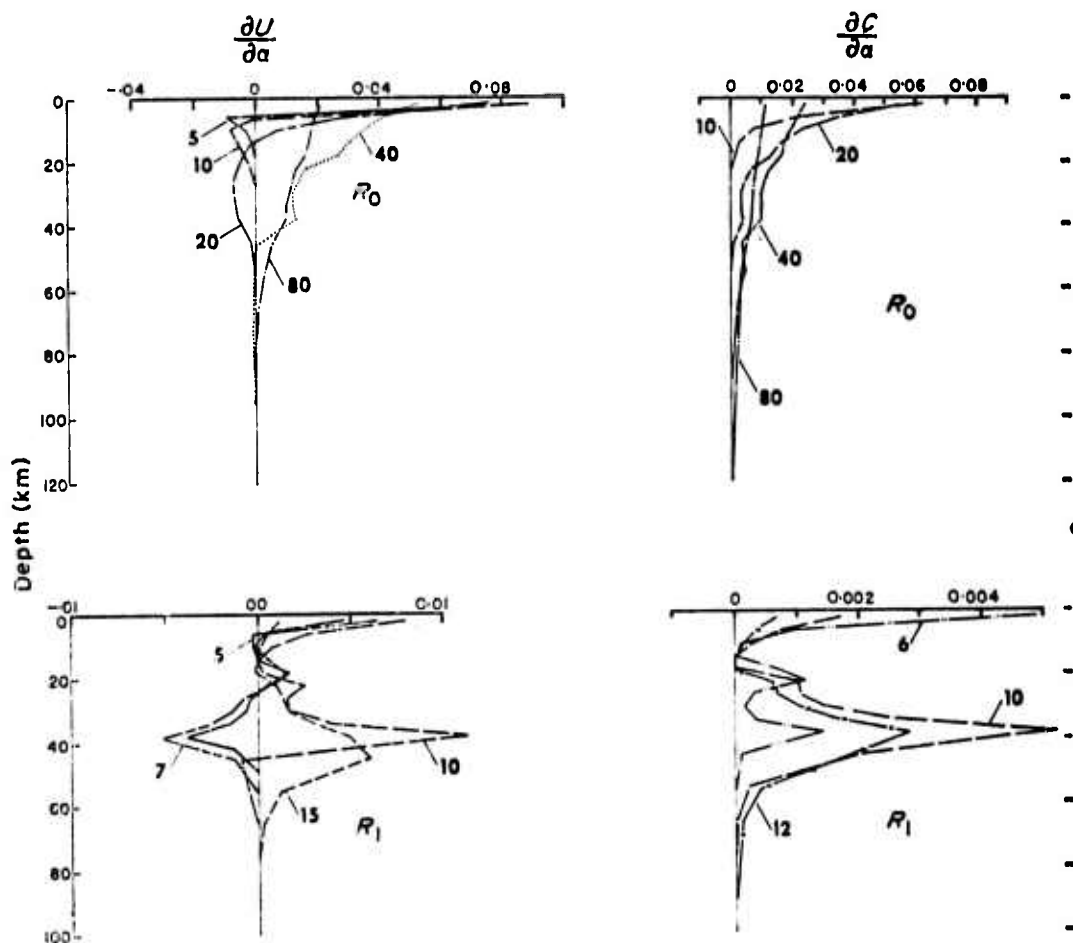


FIG. 11. Selected partial derivatives of phase and group velocities with respect to compressional velocity for shield model.

is the variable to be eliminated is shown on the left. The curves on the right show the results when the role of the two variables is reversed. The figures show that, in spite of the differences in magnitude of their partial derivatives, the two variables can be separated effectively within the crust. The dependence on the variable which is to be eliminated (dashed line) is much smaller than the dependence on the desired variable (solid line). In the upper mantle, however, the separation is much less effective, and a strong correlation between the two variables is apparent, in agreement with the results of the previous section. The decrease of the partial derivatives with depth, especially those associated with the density for the higher modes, is the primary cause of these difficulties. It would seem that it is possible to solve for both shear velocity and density within the crust if a set of fundamental and higher mode observations with the specified measurement errors is available. It must be remembered, however, that shear velocity and density are not completely independent variables and their ratio must fall within the bounds characteristic of common rock types. Therefore, if an inversion yielded models with petrologically unreasonable pairs of shear velocity and density values, one ought to look for inconsistencies and errors in the data instead of accepting the results. In conclusion, the partial derivatives seem to permit the determination of shear velocity and density independently, but the results are subject to petrological constraints.

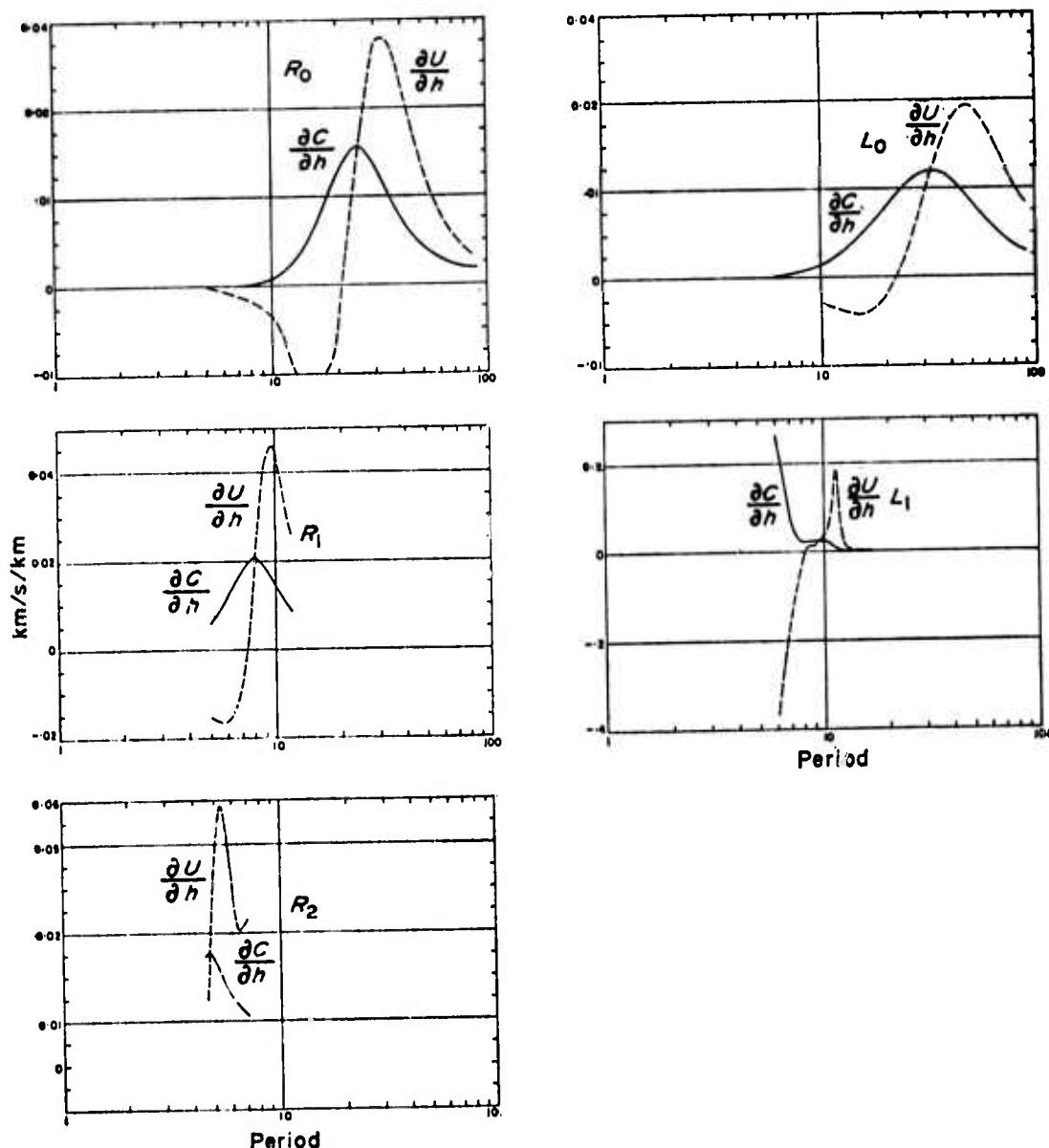


FIG. 12. Changes in phase and group velocity for shield model caused by a 1 km upward displacement of the Mohorovičić discontinuity.

#### Shear velocity vs. compressional velocity

It is apparent from a comparison of Fig. 11 with Figs 7 and 8 that the sensitivity of the fundamental Rayleigh mode to changes in compressional velocity decreases faster with depth than the derivatives with respect to shear velocity, and that the values for compressional waves are considerably smaller than those for the shear waves. This justifies the use of surface wave measurements for the determination of the shear velocity alone. The partial derivatives of the higher mode Rayleigh waves with respect to compressional velocities are even smaller than those for the fundamental Rayleigh mode. The Love modes are insensitive to compressional velocities. Therefore, the comparison of Love modes and higher Rayleigh modes with the fundamental Rayleigh mode holds the promise of detecting changes in  $P$  velocities in the upper layers, especially in the crust. Numerical experiments using partial derivatives with respect to shear and compressional velocities show that separation of the compressional velocity from the shear velocity can only be achieved at a high cost in resolution. The delta functions approximations, calculated with the compressional velocity as the

Table 2

*Observational errors associated with group velocities for calculation of resolution and separation between density and shear velocity in the crust*

Fundamental Love		Fundamental Rayleigh	
Period	S.D.	Period	S.D.
(s)	(km s <sup>-1</sup> )	(s)	(km s <sup>-1</sup> )
5.0	0.025	5.5	0.02
6.9	0.025	7.0	0.02
8.6	0.025	8.5	0.02
10.7	0.025	10.5	0.02
13.5	0.025	13.5	0.02
16.8	0.03	16.5	0.025
21.0	0.03	20.0	0.025
26.0	0.04	26.0	0.03
32.7	0.05	32.0	0.04
41.0	0.05	40.0	0.04
51.2	0.05	52.0	0.04
64.0	0.06	64.0	0.06
80.0	0.07	80.0	0.06
First higher Love		First higher Rayleigh	
Period	S.D.	Period	S.D.
(s)	(km s <sup>-1</sup> )	(s)	(km s <sup>-1</sup> )
9.6	0.05	3.15	0.03
12.0	0.04	3.93	0.03
15.0	0.05	5.0	0.03
		6.14	0.03
		7.5	0.03
		9.6	0.05
		12.0	0.05
		15.0	0.05

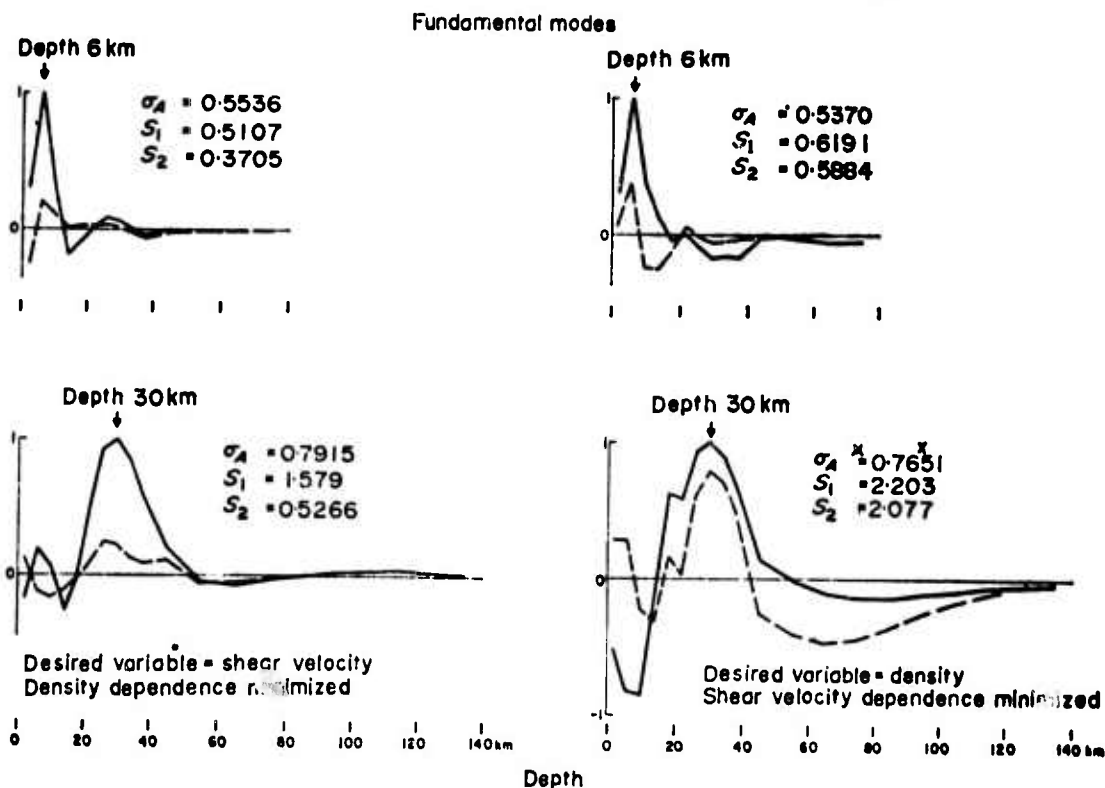


FIG. 13. Delta function approximations for *fundamental mode* observations having errors as given in Table 2. Solid lines show the dependences of the particular linear combinations on the desired variable (shear velocity at the left, density at the right); dashed line shows the dependences on the undesired variable. This figure illustrates that density can be only poorly separated from shear velocity in the lower crust and upper mantle.

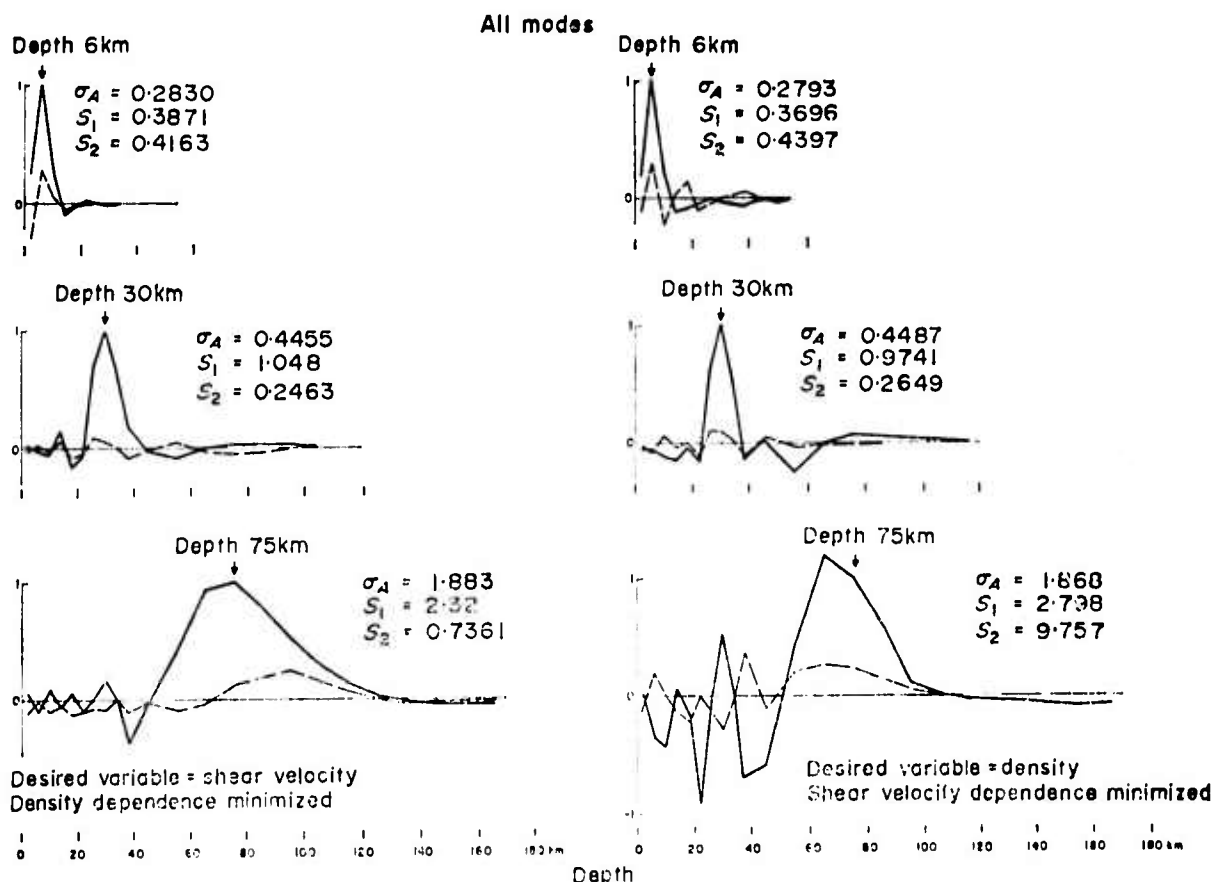


FIG. 14. Delta function approximations obtained for dispersion data having the errors in Table 2. The figure illustrates that the variables can be separated fairly well when *higher mode* data are included.

desired variable, indicate that although the dependence on shear velocity can be made very small for some linear combinations, the resolution in compressional velocity becomes poor and the standard error of the linear combination representing the compressional velocity estimates becomes large. A model with thick layers, for instance with a single-layered crust, may require an adjustment in compressional velocity for a proper fit to the data, provided that the density values are correct. Such a case, however, is not realistic. The compressional velocity is related to shear velocity through the Poisson's ratio appropriate to the rock types in the crust and upper mantle, and the range of possible ratios is very limited.

#### *Partial derivatives for crustal thickness changes*

Calculations of derivatives which show the effects of changes in the depth of the Mohorovičić discontinuity were performed, in addition to those discussed above, which show the effects of changes in the physical parameters of the layers. Fig. 12 shows the changes in phase velocity and group velocity for various modes for a 1 km upward displacement of the Mohorovičić discontinuity.

These curves show that, in general, group velocities are more sensitive than phase velocities to changes in the thickness of the crust. Large values of the 'thickness partial derivatives'  $\partial U/\partial h$  correspond to the steep portions of the group velocity curves, while the values of the phase velocity derivatives  $\partial C/\partial h$  are smaller. The absolute values of these thickness partial derivatives are greater for the higher modes since they are characterized by more abruptly changing phase and group velocity curves. This behaviour is similar to that of the derivatives discussed above.

## 5. Inversion

### *An algorithm for inversion*

It was found, during the course of the general discussion of the linear combinations of the observations in Paper I and in the papers by Backus & Gilbert (1968, 1970), that the resolution with depth, or the vertical extent of the approximate delta functions, can be specified within certain limits, and that the variances of the resulting estimators of the unknown parameters are approximately related to the inverse of the resolution specified. In particular, one can specify the minimum wavelength for each depth  $\lambda(z)$  and set up solutions such that they contain no wavelengths shorter than those specified. Alternatively, one can synthesize a solution by linearly adding functions of depth already possessing this property. The differences between the observations and calculations for an initial model, designated as  $C_i$ , can be written as an integral, if continuous functions are used for the derivatives instead of using a set of derivatives with respect to the layer parameters.

$$C_i = \int_a^b P_i(z) \delta p(z) dz, \quad i = 1, \dots, N, \quad (\text{A1})$$

where  $\delta p(z)$  is the desired change of the unknown variable  $p(z)$  relative to the initial model, and  $a$  and  $b$  span the depth range of interest.  $P_i(z)$  is the partial derivative

$$P_i(z) = \frac{\partial C_i}{\partial p(z)}. \quad (\text{A1.1})$$

It is assumed that  $\delta p(z)$  can be expressed as a sum of orthogonal functions  $\Phi_n(z)$ .

Thus

$$\delta p(z) = \sum_{n=1}^M a_n \Phi_n(z). \quad (\text{A1.2})$$

Substituting this into expression (A1) one obtains

$$\sum_{n=1}^M a_n \int_a^b P_i(z) \Phi_n(z) dz = C_i, \quad i = 1, N. \quad (\text{A1.3})$$

The least squares normal equations then become

$$\sum_{n=1}^M a_n \sum_{i=1}^N A_{in} A_{ip} = \sum_{i=1}^N C_i A_{ip}, \quad (\text{A2})$$

or, in matrix notation

$$\bar{a} D = \bar{C} A, \quad \text{with } D = A A^T \quad (\text{A2.1})$$

In (A2)

$$A_{in} = \int_a^b P_i(z) \Phi_n(z) dz. \quad (\text{A3})$$

It is necessary to ascertain that the solution  $\delta p(z)$  fits the observations and that it does not have an excessive variance after it has been obtained by solving equation (A2). The solutions of (A2) are linear combinations of the observations, and the variance of the total solution can be easily derived. Let the  $M \times N$  matrix  $B$  denote

the set of coefficients of the observations used to derive the coefficients  $a_n$  in the least squares process

$$a_n = \sum_{i=1}^M B_{ni} C_i. \quad (\text{A4})$$

In this expression, the matrix having elements  $B_{ij}$  is

$$B = AD^{-1}. \quad (\text{A4.1})$$

This gives

$$\text{cov}(a_n, a_m) = \sum_{j=1}^M B_{nj} B_{mj} \text{cov}(C_i, C_j). \quad (\text{A5})$$

If the observational errors are independent, (A5) can be written

$$\text{cov}(a_n, a_m) = \sum_{i=1}^M B_{ni} B_{mi} \text{var } C_i. \quad (\text{A5.1})$$

The amplitude of the total solution is in turn a linear combination of the coefficients  $a_n$  multiplied with the functions  $\Phi(z)$ . Therefore the variance of  $\delta p(z)$  will become

$$\text{var}\{\delta p(z)\} = \sum_{n=1}^M \sum_{m=1}^M \Phi_n(z) \Phi_m(z) \text{cov}(a_n, a_m). \quad (\text{A5.2})$$

This error estimate is based on an *a priori* estimate of measurement errors, and does not include the effect of possible internal inconsistencies in the data. Such inconsistencies can be quite serious, as will be seen later. Moreover, if the *a priori* error estimates are too low, the results may give a false illusion of high accuracy. Therefore, after the solution is obtained, the differences  $\epsilon_i$  between the observations and the values of observations extrapolated using the solution must be within reasonable limits. If several of the  $\epsilon_i^2$  are larger than, say  $4 \text{ var } C_i$  the following possibilities exist: the *a priori* error estimates are too low, the data set is internally inconsistent (no model can satisfy the data), or the model is not adequately parameterized. The last of these possibilities includes the inadequacy of the model to be fitted, for instance fitting of an isotropic layered model to data taken in a region where anisotropic layers are present, or the use of too few or inappropriate parameters.

It is desirable to weight the error terms in the least squares process, if the errors associated with the various measurements are uncorrelated and unequal. Thus instead of minimizing the sum of the squares of error terms one can minimize the sum

$$\sum_{i=1}^M \frac{\epsilon_i^2}{\text{var } C_i} = \sum_{i=1}^M X_i \epsilon_i^2, \quad X_i = \frac{1}{\text{var } C_i}, \quad (\text{A6})$$

which would provide the best fit to the most accurate observations and would tend to ignore the most inaccurate measurements in the data set. Weighting will yield normal equations of the form

$$\sum_{n=1}^M a_n \left( \sum_{i=1}^M A_{in} A_{ip} X_i \right) = \left( \sum_{i=1}^M A_{ip} C_i X_i \right). \quad (\text{A7})$$

The truncated series solution obtained will be optimum in the rms sense under the limitations imposed by the finite number of  $\Phi_n$  (Lanczos 1956), if the functions  $\Phi_n$

are chosen to be orthogonal. The idea of using orthogonal functions to obtain inverses of geophysical data was first explored by Wiggins (1970, verbal communication). Methods of this sort can be effectively used for building up solutions for relatively large depth ranges having no known discontinuities, as may be the case in the middle and lower portions of the Earth's mantle. The functions  $\Phi_n$  must be specified in accordance with limitations of the model at shallower depths where the range of possible solutions is seriously limited. For instance, while inverting short and intermediate period surface wave data, one must be careful not to violate seismic refraction results from the same area. Therefore,  $\Phi_n$  must be chosen such that the approximate depths and head wave velocities associated with major interfaces must retain their directly measured values throughout the process of inversion.

Some of the formulae and expressions derived above will be used in the following section but no attempt will be made to build up solutions from orthogonal functions. The integrals (A3) will be replaced by weighted sums of partial derivatives with respect to parameters in discrete layers.

## 6. Inversion of multi-mode surface wave dispersion data

Two sets of multi-mode surface wave observations for shield areas were used in the first application of this inversion method to studies of the crust and upper mantle. One set of data was previously reported by Bloch *et al.* (1969) for Southern Africa. The other data set is a collection of seismic results, including surface wave phase and group velocities and refraction results for Fennoscandia. The previous sections have discussed the difficulties associated with attempts to separate compressional velocity and density from shear velocity, as well as those which may arise from studies of the shear velocity alone. For these reasons, it has been assumed in this section that the changes in  $P$  velocity may be associated with a Poisson's ratio of 0.25, and that the density-compressional velocity relationship follows the average slope of the Nafe-Drake empirical relationship (in Talwani, Sutton & Worzel 1959) in the compressional velocity range 6–8 km s<sup>-1</sup>. These relations may be effected by multiplying the partial derivatives with respect to densities and  $P$  velocities by the constants 0.43 and 1.733 and adding them to the shear velocity partial derivatives. The net effect of such corrections is small, because of the lower absolute values of the density and compressional velocity partials.

The model for each inversion was subdivided into depth ranges which were separated by major interfaces, such as the Conrad and Mohorovičić discontinuities. The changes in shear velocity as functions of depth were required to follow the pre-defined functions  $\Phi(z)$  within each of the specified depth ranges. Since the partial derivatives are discrete functions of depth, it is implied that in order to evaluate the integral (A3), it is necessary to form weighted sums of the partial derivatives with respect to depth.

$$\frac{\partial C_k}{\partial \Gamma_l} = \sum_{i=1}^K v_{ii} \frac{\partial C_k}{\partial \beta_i} \quad k = 1, N. \quad (\text{A8})$$

Where  $v_{ii}$  are constant coefficients,  $\beta_i$  are the shear velocities (linked to the compressional velocities and densities in the above manner), and  $C_k$  is the  $k$ -th observation.  $\Gamma_l$  is a new parameter which describes the amplitude of  $\Phi(z)$ .

Partial derivatives with respect to the depth of the Mohorovičić discontinuity permitted the depth of this interface to be used as an additional parameter in the inversion.

A wide variety of constraints can be imposed on the model by choosing the functions  $\phi(z)$  appropriately. Several thin layers may be lumped together by adding up partial derivatives of the observations associated with them. It is possible to avoid

instability by constraining the model so as to preclude parameter changes with short vertical wave lengths. Parameter changes in thick layers or linear changes with depth (stair case) or some combinations of both were permitted in most of the inversions. Parameters can be held constant in certain layers by defining the discrete equivalents of  $v_{II}$  to be zero in certain layers. Such restrictions are desirable if known values of particular head wave velocities are to be held constant. Some of the solutions were computed with thin layers in order to see the effects of incipient instability of the inversion process on the resulting model.

The resolving lengths of the resulting models are approximately equal to the thicknesses of the compound layers where the velocities are constrained to be constant or linearly changing. The resolving length does not exceed a few layer thicknesses for the relatively unconstrained models. The concept of resolving length does not apply for models where some velocities were held constant, and no comparison with previous results (e.g. Der *et al.* 1970) is meaningful.

### Results for Southern Africa

The data set previously reported by Bloch *et al.* (1969) was used as a test case of the present inversion method. This data set consists of group velocity observations for fundamental and first-higher Rayleigh and Love modes for the Kariba-Pretoria path and phase velocity observations for the Pretoria-Bulawayo path. In addition, second higher mode Rayleigh wave observations were also included in the data. The published crustal model (*ibid*) exhibits a gradual increase of shear velocity in the crust and an increase of velocity at about 70 km depth in the mantle. This published model exhibits two crustal low-velocity layers.

Fig. 15 shows several inversions which were obtained using the published data and various constraints. The standard deviations of the resulting shear velocity estimates are indicated by horizontal bars for each subsection where the shear velocity remained constant. The standard deviation for the depth of the Mohorovičić discontinuity is shown by a vertical bar. The model PRE-BUL 1 was subdivided into thick layers, while model PRE-BUL 2 was constrained such that only uniform values and uniformly increasing changes were permitted in the depth ranges 0-20 and 20-40 k. PRE-BUL 3 was relatively unconstrained. Two of these models show velocity reversals with depth. These reversals, however, are not very significant if one considers the standard deviations of the inversion model. There must be some increase of shear velocity within the upper 100 km of the mantle according to the

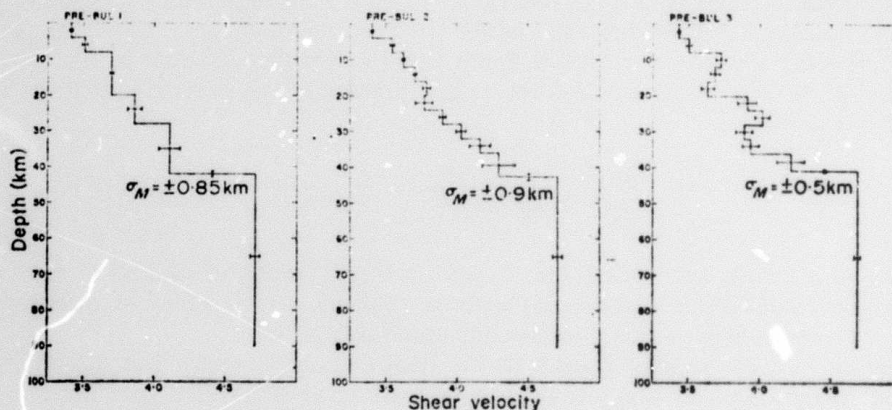


FIG. 15. Inversion results obtained with a set of dispersion data for southern Africa (after Bloch *et al.*, 1969). Estimated standard deviations of shear velocities are indicated by horizontal bars. Standard deviation for depth of the Mohorovičić discontinuity is shown by a vertical bar.

present results, but not much can be said about the details of such an increase.

Each of the inversion models fits the data roughly as well as the others, but the basic discrepancy between the first higher Love mode and the remainder of the data set is still a serious difficulty, as was noted by the original authors. This discrepancy can be resolved by including narrow low-shear-velocity layers in the upper mantle (Bloch *et al.* 1969), but other explanations are also possible, as indicated in the discussion below.

An increase in the Moho depth is also required by all the inversion models, although it never increased to 45 km as reported by Bloch *et al.* (1969).

In addition to the serious disagreement for the first higher Love mode noted above, small discrepancies persist for the higher Rayleigh modes after the inversions are completed. The internal inconsistency of this data set can be explained by the differences in path for the group and phase velocity measurements, the possibility that some of the higher modes observed were generated at structural boundaries between the epicentre and the receivers, or that the observations include a partially unseparated mixture of higher modes (James 1971). In view of all of these discrepancies, only shear velocity adjustments were considered in these inversions.

#### *Interpretation of refraction and dispersion measurements from the Scandinavian Shield*

A set of dispersion measurements for Scandinavia was inverted in order to compare the results from Southern Africa with those for another shield area. The data for Scandinavia consist primarily of fundamental mode Rayleigh and Love wave phase and group velocities, but a limited set of phase velocity observations are also available for the first higher Rayleigh and Love modes. The entire set of data is pertinent to the central part of Scandinavia, which is apparently characterized by a high degree of lateral uniformity of the velocity and thickness for the major crustal layers. The seismic data for this area also include a fairly extensive set of refraction measurements which provide important constraints upon the resulting solutions. The following brief summary of the published seismic results may be more easily understood with the help of the simplified map in Fig. 16, in which the shaded area indicates the region covered by the shield. It also located several of the more important refraction lines and inter-station dispersion paths.

#### *Seismic refraction studies in Scandinavia*

Numerous seismic refraction studies have been conducted in the Scandinavian shield area, especially during the past few years. Sellevoll & Penttillä (1964) report an unreversed refraction profile in the northern part of Norway and Finland (broken line AA in Fig. 16). The interpretation indicates a 14 km granitic layer underlain by a 19 km basaltic crustal layer, leading to a total crustal thickness of 33 km, which appears to be a fairly typical thickness for the edge of the shield. The  $P$  wave refracted phases have the following apparent velocities:  $P_g \sim 5.95 \text{ km s}^{-1}$ ,  $P_b \sim 6.7 \text{ km s}^{-1}$  and  $P_n \sim 8.18 \text{ km s}^{-1}$ . This refraction profile ran south-eastward from shots fired in the Norwegian Sea off Tromsø on the north-western Norwegian Coast, extended through the Caledonian mountain chain in Norway, and continued into the Pre-Cambrian area in northern Finland.

Noponen, *et al.* (1967) report results from an unreversed EW profile (CC) from the Gulf of Bothnia into the southern part of Finland. Three crustal layers were found, with thicknesses of 12.2, 18 and 11.8 km, and  $P$  velocities of 6.07, 6.51 and  $6.64 \text{ km s}^{-1}$ , respectively. The  $P_n$  arrivals from the upper mantle at a depth of 42 km had a velocity of  $8.03 \text{ km s}^{-1}$ . This value of crustal thickness appears to be more typical of the central portions of the shield.

Dahlman (1967a) presents an interpretation of average travel times for crustal waves from several explosions in Norway as recorded at many of the seismic stations

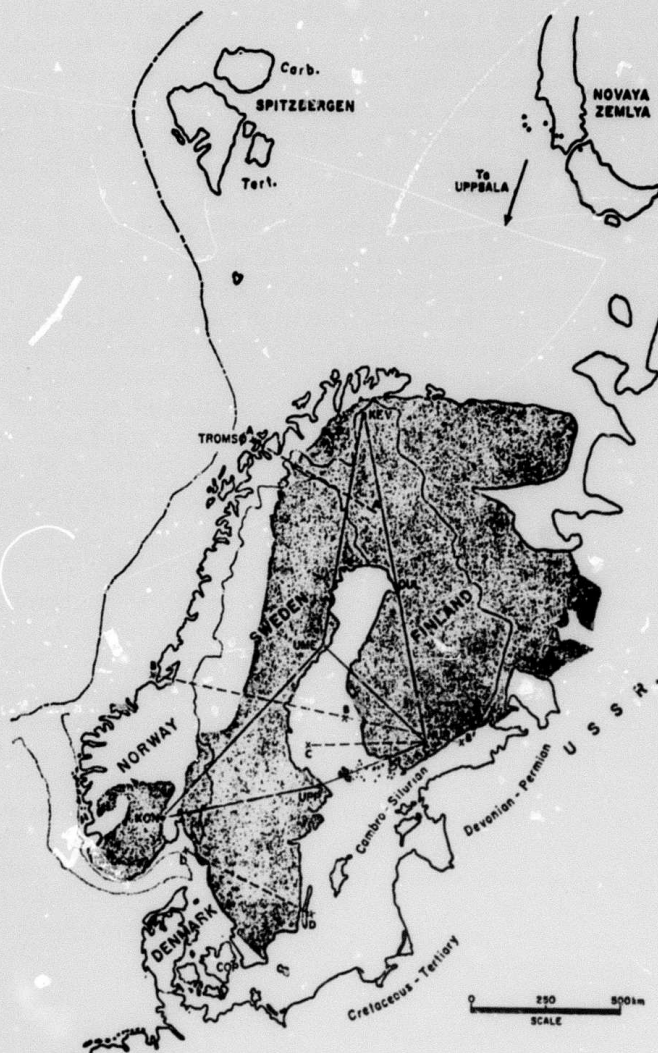


FIG. 16. Refraction profiles (broken lines) for the Scandinavian shield, used for derivation of the initial model SCAN. Interstation paths (solid lines), used for surface wave dispersion measurements. The path from Novaya Zemlya to Uppsala is also indicated. See text.

operating in Sweden and Finland. He found a granitic layer having a thickness of 12 km, which is associated with velocities,  $P_g = 5.98 \text{ km s}^{-1}$  and  $S_g = 3.54 \text{ km s}^{-1}$ . Beneath this, the interpretation indicates a basaltic layer with a thickness of 27 km, and velocities  $P_b = 6.35 \text{ km s}^{-1}$  and  $S_b = 3.79 \text{ km s}^{-1}$ . The subcrustal refraction velocities from an average depth of 39 km were found to be  $8.29 \text{ km s}^{-1}$  for  $P_n$  and  $4.70 \text{ km s}^{-1}$  for  $S_n$ . This model was found to be in good agreement with travel times reported subsequently for some test explosions in western Sweden (Dahlman 1967b).

Sellevoll & Pomeroy (1968) made an extensive study of travel times from explosions in Scandinavia. They found the following crustal and upper mantle velocities  $P_g = 6.1$ ,  $P_b = 6.59$ ,  $P_n = 8.18$ ,  $S_g = 3.58$ ,  $S_b = 3.77$  and  $S_n = 4.63 \text{ km s}^{-1}$ .

Sellevoll (1968) reports a number of seismic refraction profiles in western Scandinavia. These profiles show crustal thicknesses ranging between 30 and 35 km in southern Norway and also in the north-western coastal region of Norway. Both



granitic and basaltic layers are present, with  $P$  velocities of 6.0 and 6.51 km s<sup>-1</sup>, respectively, in southern Norway. The  $P_n$  velocity was found to be 8.05 km s<sup>-1</sup> in the same region.

Vogel & Lund (1970) report a combined interpretation of seismic refraction and gravity data for a trans-Scandinavian profile (broken line BB) which crossed Norway, central Sweden and part of the Gulf of Bothnia in a WNW-ESE direction, and continued across southern Finland toward the shotpoint B'. Their results show a crust which is about 43 km thick on the average. They distinguished three to four crustal layers, with a fairly high  $P$  velocity,  $\sim 7.1$  km s<sup>-1</sup>, in the deepest crustal layer. The subcrustal  $P$  wave velocity was found to be 8.13 km s<sup>-1</sup>.

The Moho profile obtained by arrival time residuals indicates a root for the Caledonian mountain range in west-central Norway. A reasonable agreement between the theoretically computed Bouguer anomaly and the observed values were found for a density contrast of 0.5 g cm<sup>-3</sup> between the crust and upper mantle.

This list of refraction results for Scandinavia is by no means exhaustive. The results quoted above show a rather uniform structure for most of Scandinavia, both in the crustal thicknesses and in the body wave velocities for the intermediate layers of the crust. Peripheral areas of the shield retain similar body wave velocities, but the crustal thicknesses are smaller than those for the central portions of Scandinavia which are most characteristic of the shield. Such peripheral areas include the coastal regions of Norway, and all of Denmark. For these reasons the refraction results for the shield area from the trans-Scandinavian profiles BBB' and DD as interpreted by Vogel & Lund (1970), and the earlier line across southern Finland (CC) reported by Noponen *et al.* (1967) served as the basis of an initial model, SCAN, to be discussed below.

#### *Multi-mode surface wave dispersion data*

Dispersion data for this study were collected from the published papers of several authors. Fundamental mode Rayleigh and Love wave phase velocities were taken from Noponen (1966), who measured interstation phase velocities along a NS path across Finland, using data from epicentres in Greece recorded by the Finnish stations NUR, OUL, and KEV. Group velocities for the same path were obtained by Noponen *et al.* (1967), by fitting polynomials to peak and trough arrival times and taking interstation differences of the group arrival times. Although phase and group velocities are not independent, both sets of data were used to help determine the final models. The data are shown in Figs 17 and 18, along with calculated values for the initial model SCAN. Use of this larger set of data, although it is redundant, will still increase the reliability of the final model and help to insure that the solution remains within the error limits for both group and phase velocities. Higher mode phase velocities between various Scandinavian stations (KEV, NUR, UME, UPP, KON and COP, indicated in Fig. 16) were obtained by Crampin (1964) for the first higher Rayleigh and Love modes. These data, and corresponding higher mode calculations for the initial model SCAN, are presented in Fig. 19.

At first, an attempt was made to include some higher mode group velocity data obtained by Crampin (1966b) along a path from Novaya Zemlya to Uppsala as shown on the map, since both the published seismograms, reproduced in Fig. 20, and the derived dispersion curves were similar to other results for Scandinavia. These data, although they strongly resemble the continental dispersion for this area, were found by the program to be inconsistent with the rest of the data set for Scandinavia, and had to be discarded. It appears likely that the first part of the path from Novaya Zemlya to Uppsala lies outside the northern edge of the shield, where the crustal thickness is smaller than it is in the central part of Sweden and Finland. The authors did not expect the inversion method to be so sensitive to small differences in geologic

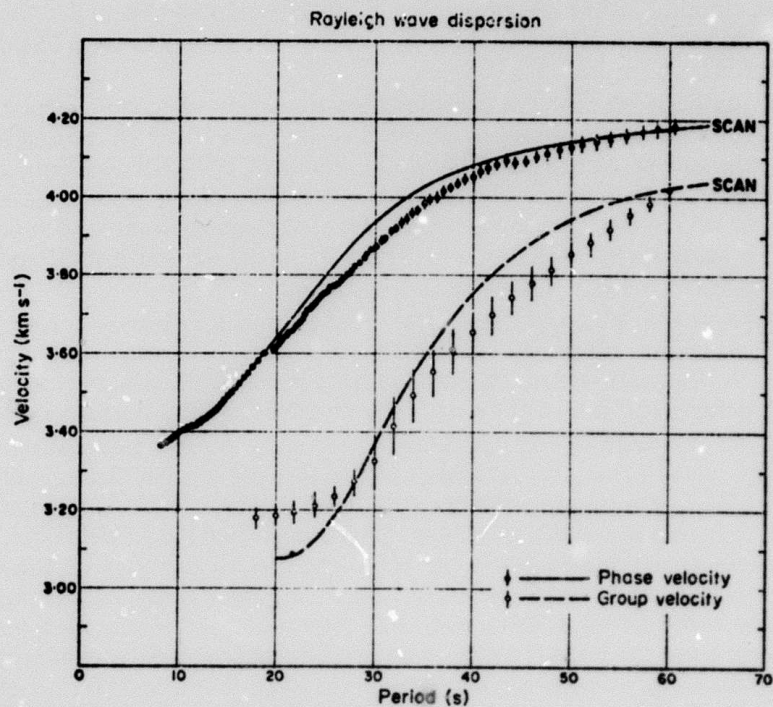


**FIG. 17.** Fundamental Rayleigh wave dispersion for the Scandinavian shield, after Noponen *et al.* (1967). Vertical bars show standard deviations as estimated by the above authors. Dispersion computed for model SCAN is shown for comparison.

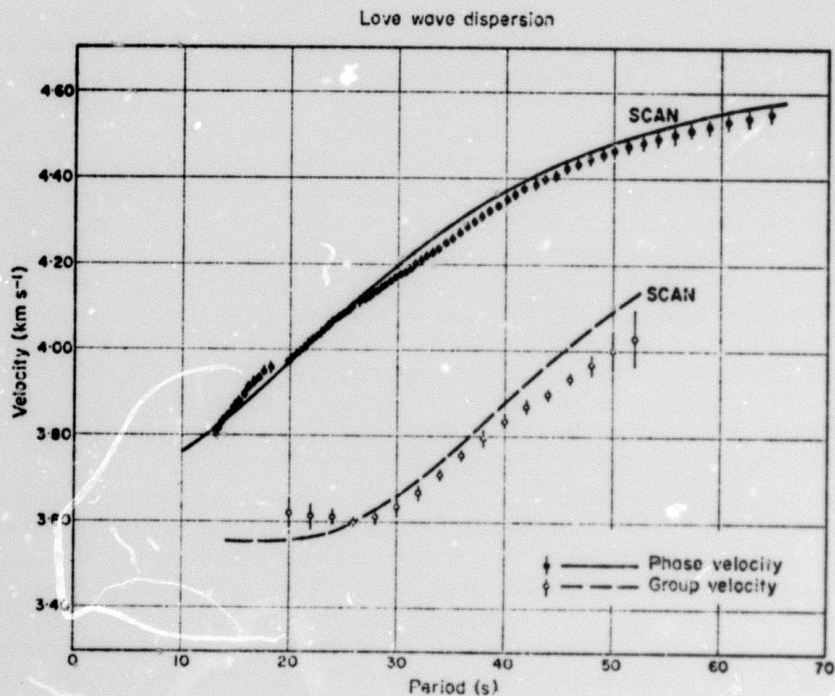


**FIG. 18.** Fundamental Love wave dispersion for the Scandinavian shield after Noponen *et al.* (1967) compared to dispersion computed for model SCAN.

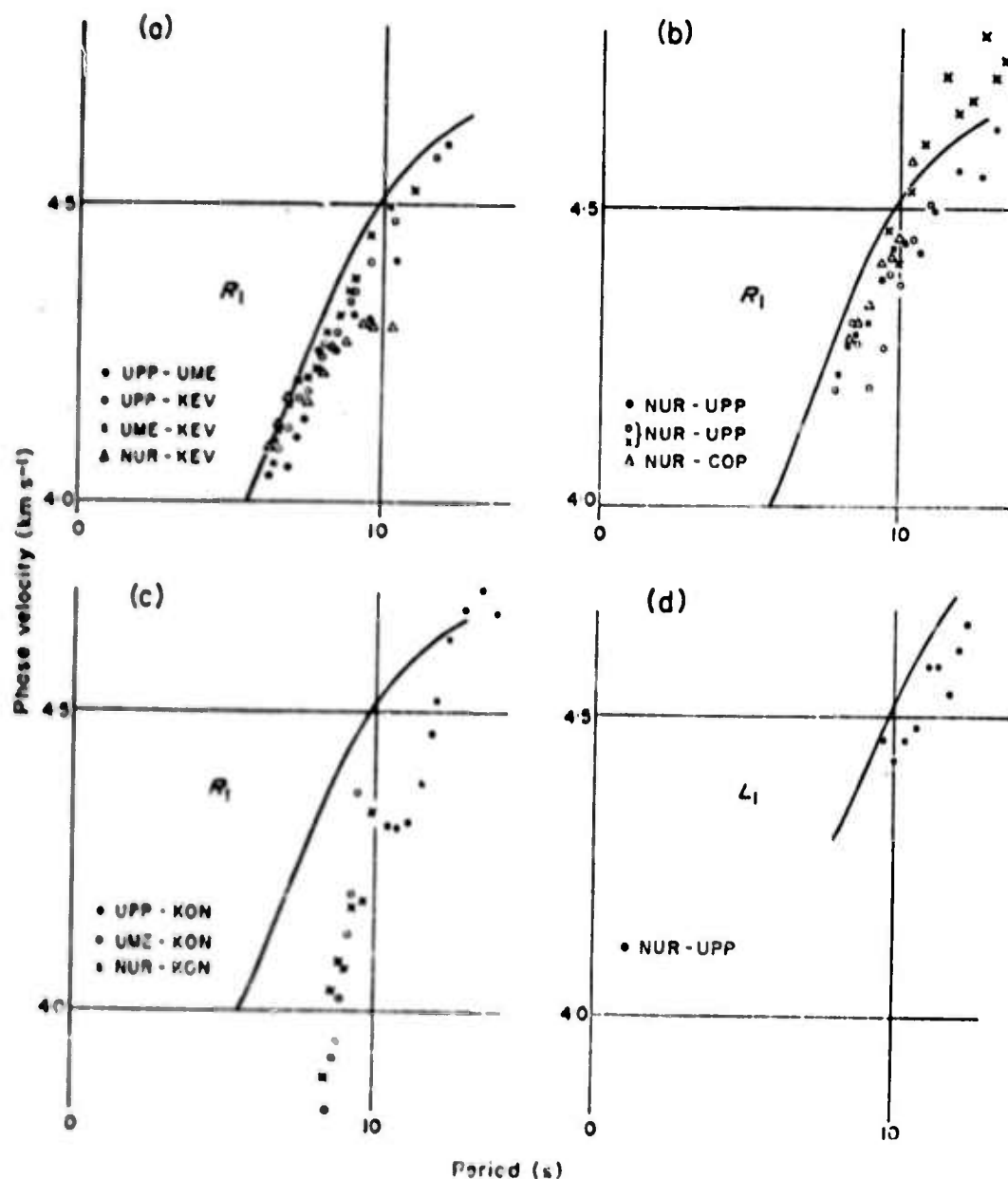


FIG. 19. Higher mode phase velocity observations after Crampin (1964) compared to dispersion computed for model SCAN.

region, but are encouraged that lateral variations in the crust and upper mantle may be delineated in this way.

An initial model, designated SCAN, was assumed for the process of inversion. The layer thicknesses and velocities in this model were chosen such that they corresponded as closely as possible to averaged refraction results in the central portion of Fennoscandia. The subcrustal velocities were taken to be the same as those of the initial model used by Bloch *et al.* (1969) for the inversion of multi-mode surface wave data in southern Africa. This upper mantle model includes an upper mantle low-velocity layer beginning at a depth of 120 km, and a sharp increase of velocity below the low-velocity channel, at a depth of 400 km. The parameters for model SCAN are shown in Table 3.

Figs 17, 18 and 19 show the original data points used in this study. The dispersion computed for the model SCAN is also included for comparison. Vertical bars across the data points show the mean square error (variance) ranges, as estimated by the

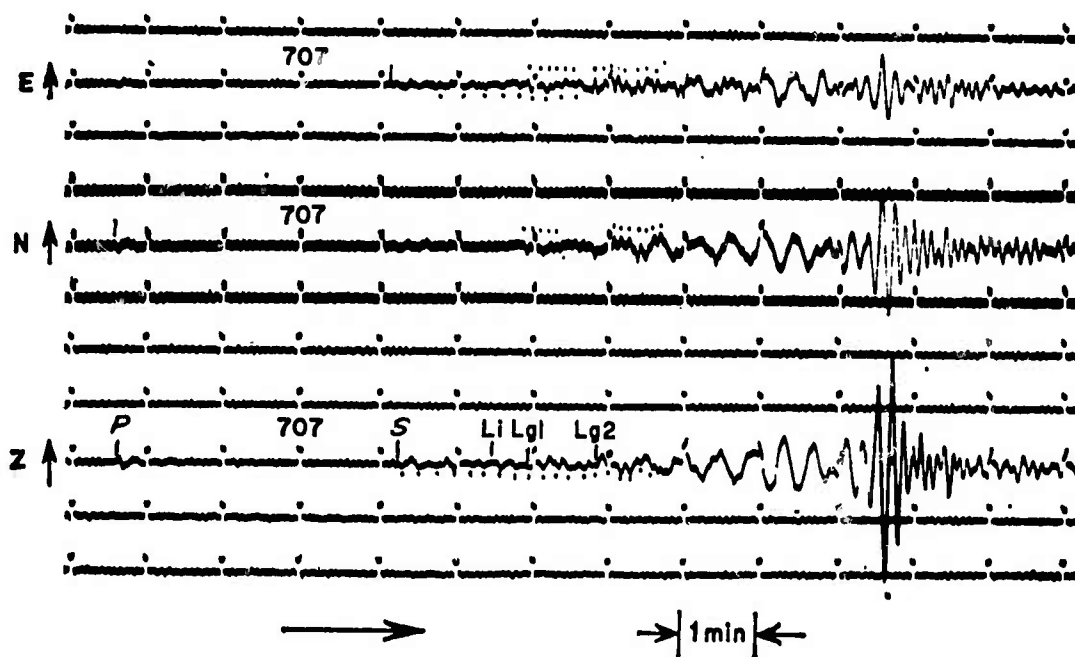


FIG. 20. Uppsala Press-Ewing long-period recordings of the nuclear event of 1961 October 6 detonated off the coast of Novaya Zemlya, at an azimuth of  $28.4^\circ$  and a distance of 2160 km from Uppsala. The higher and fundamental mode surface waves are exceptionally clear, and exhibit typically continental dispersion. (After Crampin (1966b), reproduced with permission of the *Journal of Geophysical Research*.)

Table 3

## Model SCAN

Depth to top of layer (km)	Thickness (km)	P velocity ( $\text{km s}^{-1}$ )	S velocity ( $\text{km s}^{-1}$ )	Density ( $\text{g cm}^{-3}$ )	
0	12	6.1	3.58	2.7	
12	16	6.51	3.76	2.8	
28	12	6.6	3.8	2.9	
40	60	8.1	4.7	3.3	
100	20	8.3	4.7	3.3	
120	20	8.3	4.55	3.4	
140	80	8.4	4.55	3.4	
220	60	8.4	4.55	3.5	
280	60	8.5	4.55	3.5	
340	20	8.5	4.7	3.6	
360	40	8.6	4.7	3.6	
400	40	9.1	5.3	3.7	
440	60	9.1	5.3	3.9	
500	180	9.2	5.4	4.1	
680	20	10.0	5.8	4.2	
700	—	11.0	6.3	4.3	

Crust  
Upper  
mantle

Table 4

*Periods, velocities and standard deviations of dispersion observations used for the inversion of Scandinavian data*

Fundamental Love			Fundamental Rayleigh		
Period (s)	Group velocity	S.D. (km s <sup>-1</sup> )	Period (s)	Group velocity	S.D. (km s <sup>-1</sup> )
20.0	3.62	±0.03	20.0	3.19	±0.04
26.0	3.60	0.03	26.0	3.23	0.04
32.7	3.69	0.02	32.0	3.41	0.06
41.0	3.85	0.02	40.0	3.65	0.07
51.4	4.02	0.08	52.0	3.89	0.07
			64.0	4.04	0.06
Phase velocity			Phase velocity		
13.0	3.81	±0.01	13.0	3.44	±0.01
16.0	3.90	0.02	16.0	3.52	0.01
20.0	3.98	0.02	21.0	3.65	0.01
26.0	4.10	0.02	26.0	3.77	0.01
32.0	4.21	0.02	32.0	3.92	0.01
40.0	4.35	0.03	40.0	4.05	0.02
52.0	4.48	0.04	52.0	4.14	0.03
64.0	4.55	0.04	64.0	4.19	0.03
First higher Love			First higher Rayleigh		
Phase velocity			Phase velocity		
8.0	4.29	±0.05	6.0	3.98	±0.03
10.0	4.46	0.05	8.0	4.24	0.03
12.0	4.60	0.05	10.0	4.44	0.03
			12.0	4.59	0.03

12.0

original authors. In many cases it appears that the published errors may be too small, when the amount of data and the lengths of the interstation paths are considered. The observational error estimates were modified, and Table 4 shows these values as well as the dispersion observations used for inversion. Comparison of the dispersion for model SCAN with these data shows that SCAN seems to be a very good starting point for the process of inversion. Therefore, only relatively small adjustments will be necessary to achieve a good fit to the observations, giving assurance that the linearizations implicit in the foregoing theory are apparently justified in this case. The main differences between the data and the dispersion for model SCAN are the following: The observed fundamental Love mode phase velocities at long periods are smaller than those of the model; the observed fundamental Rayleigh mode phase velocities are smaller for periods near 30 s, higher mode phase velocities are in general smaller than those computed for the model; observed fundamental Love and Rayleigh mode group velocities are smaller at long periods and larger at short periods than those for model SCAN.

#### *Results for Scandinavia*

A number of models were computed which fit the data very well, and which satisfied various types of constraints on the inversion. The process of inversion was verified in two ways. The changes of the model parameters during the inversion process, leading to changes in the expected dispersion curves, were checked by using the original partial derivatives, and comparing the extrapolated dispersion curves against the values calculated for the original model; this relatively simple test was satisfied by all of the resulting models. In addition, the dispersion was recomputed for a limited set of models and compared to the extrapolations obtained indirectly. In all tested cases a very good agreement was found. The deviations between the dispersion of the inversion models and the data seldom exceed one standard deviation

Table 5

*Constraints used for inversion of Scandinavian data\**

Model	Depth ranges (km)	
SCAN BRP2	0-12	U, L
	12-16	F
	16-28	L
	20-28	U
	28-40	U, L
	40-50	F
	50-90	L
	70-90	U
	90-140	U
	140-190	U
SCAN BRP3	0-12	U
	12-28	U
	28-40	U
	40-90	U
	90-140	U
SCAN BRP4	140-190	U
	0-8	U
	8-12	U
	12-20	U
	20-28	U
	28-40	U
	40-90	U
	90-140	U
	140-190	U
SCAN BRP6	0-12	U
	12-16	F
	16-28	L
	20-28	U
	28-40	U
	40-50	F
	50-90	L
	60-90	U
	90-140	U
	140-190	U

\*F fixed value of velocity

U uniform velocity change

L linear change permitted

as it was originally estimated, and never exceed two standard deviations for any of the observations. This indicates that the internal consistency of the data set is entirely satisfactory, i.e. all of the observations pertain to the Scandinavian shield. It also indicates that the inversion procedure was able to close fairly rapidly to a stable solution, after starting from the model SCAN which is based upon refracting measurements.

A set of inversion results were obtained by using the constraints shown in Table 5. This table shows various depth ranges for each model and indicates the kind of change which was permitted within each depth range. Three types of constraints were used, each indicated by symbols.

F fixed

U Uniform velocity change permitted

L Linear change with depth is permitted

The results of several inversions of the dispersion data for Scandinavia are shown in Fig. 21. SCAN BRP2 is the least constrained of all the models, except at two of the interfaces, where the  $S_b$  and  $S_n$  velocities are held constant. This model shows the

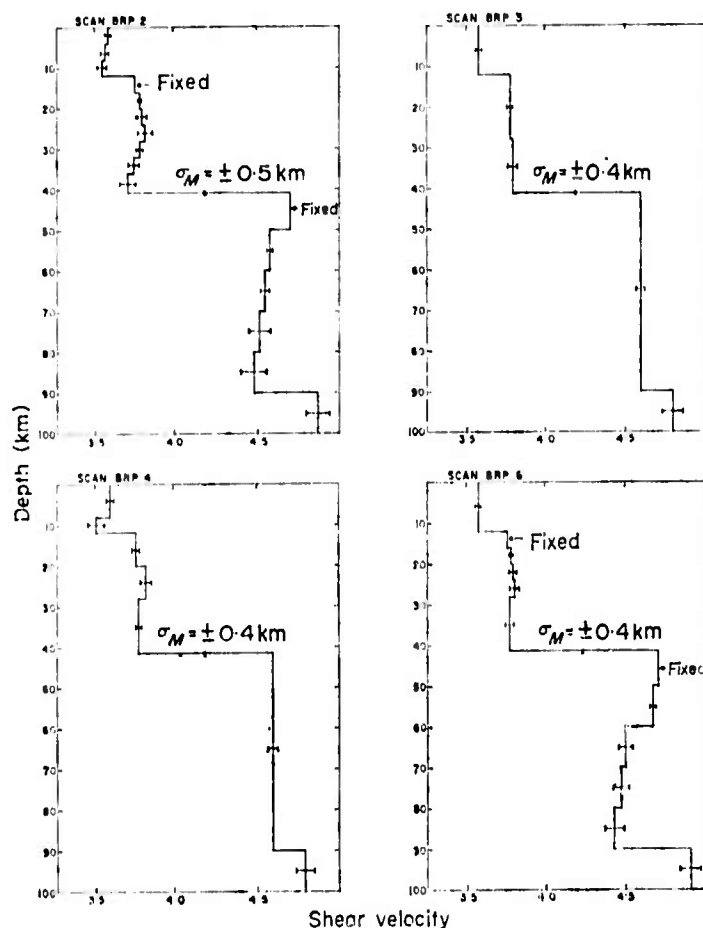


FIG. 21. Inversion results obtained for Scandinavia, using constraints on the models as shown in Table 5. Estimated standard deviations of shear velocities are indicated by horizontal bars. Vertical bar shows standard deviation for depth of the Mohorovičić discontinuity.

greatest number of inversions. The other models seem to exhibit a smoother increase of velocity with depth and seem to fit the dispersion data just as well, but they effectively ignore and are rather incompatible with much of the refraction data.

The inversion models in Fig. 21 show error bars which indicate the standard deviation of the estimates for shear velocity and Moho depth. These errors depend upon the sensitivity of the partial derivatives, upon the constraints used, and upon the error estimates for the observations, as given in Table 4. The error bars indicate approximate 68 per cent confidence limits, assuming that the distribution of the observational errors is gaussian. Two standard deviations would give about 95 per cent confidence limits, if the above assumption is valid. Strictly speaking, however, such confidence limits cannot be used since very little is known about the probability distribution functions of the errors. Nevertheless, such limits were still useful indicators of the errors of the resulting estimates, provided that the distributions of observational errors are unimodal and not extremely skewed, which is probably the case.

All the models show a slight increase of crustal thickness compared to the original estimate of 40 km. This is concordant with the refraction data, which show crustal thicknesses slightly greater than 40 km in the central portion of the Scandinavian shield.

There is a decrease of the subcrustal shear velocity from 4.7 to 4.6 km s<sup>-1</sup>, in the models for which this quantity is not constrained. If the subcrustal velocity is not changed, the inversion models require a significant decrease of shear velocity at depths

of a few tens of kilometres below the crust. The large differences between the various inversion models in this depth range indicate the low sensitivity of this data set to changes at greater depth.

Another significant feature of the inversion is the marked decrease of shear velocity in the lower crust relative to that for model SCAN; this decrease tends to obscure the deepest intracrustal interface. The velocity tends to increase in the middle portion of the crust, but the increase does not greatly exceed the errors at corresponding depths.

A velocity inversion tends to develop in the uppermost portion of the crust in models with a relatively large number of thin layers, and in models for which refraction measurements of shear velocity were used as constraints. This region constitutes the 'granitic layer' found in refraction studies. The reliability of this low-velocity layer, as indicated by the standard errors shown in Fig. 21, is not very great. It is interesting to note, however, that a widespread low velocity layer for *P* waves has been found at this depth in the continental crust (Mueller & Landisman 1966; Landisman, Mueller & Mitchell 1971).

It must be recognized that by constraining the inversion models, considerable bias was introduced and only those features which are common to all of them must be considered to be the most representative of the results. Nevertheless, there are several alternative cases which are compatible with, although not absolutely required by, the surface-wave data alone. These alternative models contain interfaces associated with certain of the shear-wave velocities which have been constrained to be equal to the observed head-wave velocities, but which also are characterized by changes in the average velocities in the layers above these refracting horizons. These velocity changes would, in general, imply alterations in the depths to the corresponding refraction horizons compared to the depths interpreted from the observed apparent velocities and intercept times. The error limits in Fig. 21 indicate, however, that these discrepancies can be reduced considerably without violating the surface wave data. The *direction* in which the velocities tend to change if the model is thus constrained is really the question of primary importance. The introduction of the observed  $S_b$  and  $S_n$  head-wave velocities leads to the inference of *shear velocity inversions* associated with each of these refractors in the resulting models. The depths and magnitudes of these inversions may be refined in the future with better data which would warrant the provision for a more complicated modelling technique. The remarkable decreases in shear velocity, inferred from the uppermost mantle on the basis of  $S_n$  observations and surface wave data, ought to correspond to observable effects in the shear-wave travel-time curve at appropriate distances. The low sensitivity of the present set of short-period surface-wave data to details of the model at upper mantle depths almost surely means that some features will require alteration when better data become available. In brief, the present set of models were made primarily to fit the surface-wave data, while retaining the observed head-wave velocities at *approximately* the proper depth.

Basically a two layer crust with about 42 km thickness can satisfy the dispersion data reasonably well. The average subcrustal shear velocity should be about  $4.6 \text{ km s}^{-1}$  with an increase to about  $4.75 \text{ km s}^{-1}$  at a greater, but unspecified depth in the range 70–100 km. Possible velocity inversions can be present at the base of the top 'granitic' layer, and in the lowest part of the crust especially if a deeper refractor such as that given by Noponen *et al.* (1967) is assumed to exist at a depth of about 30 km. If the subcrustal shear velocity is constrained to be  $4.7 \text{ km s}^{-1}$ , which is the observed  $S_n$  velocity in Scandinavia, a decrease of shear velocity is required in the first few tens of kilometers below the crust. The velocity inversions are only significant in the light of refraction data; the surface wave data alone do not require their existence, but are compatible with them.

The models outlined above show a marked resemblance to the model UL056

presented by Noponen *et al.* (1967). The differences of shear velocity and density between the two models, while not very great, may well prove to be of significance in future detailed studies.

The compressional velocities and densities were adjusted simultaneously with the shear velocity during the inversion in order to obtain the result outlined above. This procedure did not drastically alter the results in the present case; the accuracy of the initial model derived from refraction studies and the remarkable degree of lateral uniformity in this area made the adjustments small relative to the original uncertainties of these quantities and the sensitivity of the data to them. Small changes of the densities and compressional velocities of the model would not affect the dispersion results severely. There is insufficient experience at present to warrant the conclusion that this set of conditions can be duplicated in other areas.

The inversion results presented above leave open the possibility of a low-velocity layer in the crust at a depth of about 12 km. Any other low-velocity layers in the crust must be in the deepest part of the crust. If the deeper low-velocity layer is caused by dehydration of silicates (Mitchell & Landisman 1970, 1971; Landisman *et al.* 1971) the greater depth may imply lower temperatures in the crust than in other areas where such layers have been observed at shallower depths.

Summarizing the above results, the data require a decrease of shear velocity below the crust, and some increase in the middle portion of the crust relative to the original model SCAN. A velocity inversion in the uppermost tens of kilometres of the mantle appears to be necessary if the subcrustal shear velocity is constrained to the value of  $4.7 \text{ km s}^{-1}$  observed in numerous refraction experiments in this area. Another channel may be required at the bottom of the crust. The channel bottoming at a depth of 12 km, although possible, is not strongly required by the data.

Some of the models having approximately similar constraints do not fit within the corresponding error limits shown in Fig. 21. These apparent discrepancies can be partially explained by the complicated nature of the biases introduced by various groups of roughly similar constraints, and by the distinct possibility that the *a priori* error estimates given in Table 4 may be too low. This is quite likely since the error limits are smaller than those for the more complete data set in Paper I. Therefore an increase of some error estimates by a factor of 1.5–2 could easily remove these apparent inconsistencies.

It is interesting to speculate about the significance of the low-velocity layer in the first few tens of kilometres beneath the Mohorovičić discontinuity, which appears in the solutions when the  $S_n$  velocities observed in refraction measurements are introduced as a constraint. The effective propagation of  $S_n$  to large distances within the boundaries of the normal continental plates (Molnar & Oliver 1969), may well be related to a low-velocity channel at these shallow depths in the upper mantle. Fig. 22, reproduced from the cited paper, shows areas of efficient propagation of high-frequency  $S_n$ , which include shields and other portions of the plates featured in the new global tectonics, and inefficient propagation, which correspond to tectonic regions. This speculation implies that the shear waves observed at smaller distances, with an apparent velocity of  $4.7 \text{ km s}^{-1}$ , are head waves propagating in the higher velocity 'lid' above this shallow low-velocity channel in the lithosphere; propagation to larger distances may well be attributed to a guided wave in this shallow channel. Extensive reflections from depths of about 80 km have been observed with the aid of large seismic arrays (Davies 1971), and many electrical investigations indicate a sharp drop in resistivity at depths of the same order (Fournier, Ward & Morrison 1963; Fournier 1966; Mitchell & Landisman 1971; Van Zijl 1969; Van Zijl, Hugo & DeBelloc 1971). This feature is much shallower than the main mantle low-velocity zone for shear waves, which corresponds to the low- $Q$  zone.

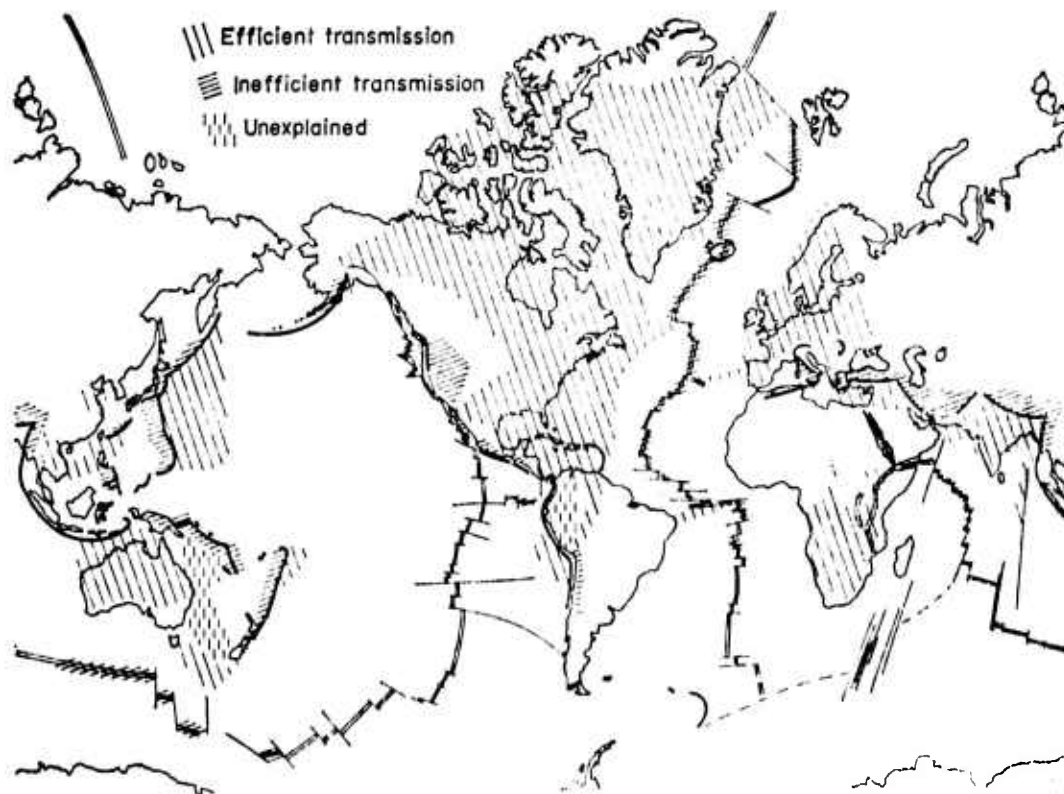


FIG. 22. Areas of efficient and inefficient propagation of high-frequency  $S_n$ . (After Molnar & Oliver (1969), with permission of the *Journal of Geophysical Research*.)  
For discussion see text.

## 7. Conclusions

A competitive relation exists between the quantities which are indicators of accuracy in the determination of a variable within the Earth, the depth resolution obtainable, and the separation from other variables which also influence the data. Improvement in any of these indicators will result in the degradation of the others. The inverse problem is therefore non-unique and an infinite set of solutions is possible, depending upon the relative importance assigned to accuracy, depth resolution, and separation of variables.

A set of free oscillation results, having errors specified by Derr (1969), was investigated. It was found that most of the depth resolution for shear waves was determined by the fundamental mode spheroidal observations. The addition of torsional modes and the limited set of commonly observed higher mode observations increased the possibility of the separation of shear velocity from density, but there was hardly any increase in the depth resolution for shear waves.

A degree of separation of shear velocity from density in the crust is theoretically possible if a set of highly accurate observations of fundamental and higher mode Rayleigh and Love wave observations is available at intermediate distances. Such data sets are, however, difficult to obtain, and the inversion usually must be confined to studies of shear velocity. The insensitivity of surface waves to compressional velocity means that alterations of this parameter can be neglected in most cases.

Inversion models with a specified resolution as a function of depth can be obtained by linearly combining the partial derivatives in order to build up solutions which are smooth functions of depth. The use of orthogonal functions for this purpose possesses certain advantages. Alternatively, as was done in this study, a suitable selection of functions can be used to constrain the inversion models, in order to satisfy conditions

imposed by data other than those included in the set of dispersion observations. The resulting models naturally will be biased by such external conditions. The accuracy of such models can be determined by using an *a priori* error estimate for the observations in the dispersion data set. It is reasonable to accept the simplest model which fits a given group of observations. Consideration of additional data tends to refine the resulting estimate.

Inversion of the dispersion data for southern Africa reported by Bloch *et al.* (1969) showed that the crustal low-velocity layers obtained, while compatible with the dispersion data, are not required by them to a statistically significant degree. Fundamental internal discrepancies also exist in the data, which make the fit very poor for the first higher Love modes. As was shown by Bloch *et al.* (1969), such discrepancies can be resolved by postulating thin low-velocity layers in the upper mantle. Other possible explanations include higher mode contamination (James 1971), mode paths used in the inversion which are near each other, but which are sufficiently different in their dispersion characteristics.

conversion  
along the path  
for some events,  
or discrepancy  
between  
propagation

Inversion of a highly consistent set of surface wave data for Scandinavia resulted in models which, on the average are similar to those previously proposed by Noponen *et al.* (1967). Consideration of refraction velocities mildly supports the concept of the sialic low-velocity layer (Mueller & Landisman 1966). A more significant crustal low-velocity layer may possibly exist in the lowermost part of the crust in Scandinavia. If such low-velocity layers are explained by a 'wet layer' caused by the dehydration of silicates, this implies that the temperatures in the crust are lower in Scandinavia than in other areas where such layers were found at shallower depths. A velocity inversion in the uppermost tens of kilometres of the upper mantle is caused by the inclusion of  $S_n$  velocities observed in refraction experiments as a constraint in the inversion process. This velocity inversion may well be characteristic of the normal continental plates, as implied by widespread observations of relatively unattenuated high-frequency  $S_n$  phases that may represent guided waves, and by observations of compressional wave reflections at narrow angles of incidence from subcrustal depths of about 80 km.

### Acknowledgments

Computer time for this study was generously furnished by the Teledyne-Geotech Company. The authors express their gratitude to Mr R. A. Arnett and Mr J. H. Whalen for permission to use the computer facilities.

This study was supported in part by the Air Force Cambridge Research Laboratories under Contract F 19628-70-C-0176, by the Office of Naval Research under Contract N00014-67-A-0310-0001, by the National Science Foundation under Grants GA-1404, GA-22706, and GA-27678, by the National Aeronautics and Space Agency under Grant NGL 44-004-001, and by departmental funds of the Geosciences Division of the University of Texas at Dallas. A small portion of the calculations were performed at the AEC Computing Center of the Courant Institute for Mathematical Sciences, New York University.

It is a pleasure to thank Mr W. Chaipayungpun and Dr B. J. Mitchell for their help with a few of the tables and figures; Dr Mitchell also participated in helpful discussions. The authors are also grateful to Dr E. Husebye, NOR SAR, Norway, Dr A. Vogel, Uppsala, and Dr O. Dahlman, FOA, Sweden, for helping the authors to obtain several of the reports used in this study.

It is a pleasure to thank Mrs Ruth Ricamore for the care and skill which she displayed during the preparation of the figures in this study.

Zoltan A. Der:  
Geotech-Teledyne Seismic  
Data Laboratory  
Alexandria, Virginia

M. Landisman:  
University of Texas at Dallas

### References

- Anderson, D. L., 1967. Latest information from seismic observations, *The Earth's Mantle*, ed. T. F. Gaskell, 355-420, Academic Press, New York.
- Alterman, Z., Jarosch, H. & Pekeris, C. L., 1961. Propagation of Rayleigh Waves in the Earth, *Geophys. J. R. astr. Soc.*, 4, 219-241.
- Backus, G. E., 1970a. Inference from inadequate and inaccurate data I, *Proc. Natl. Acad. Sci.*, 65, 1-7.
- Backus, G. E., 1970b. Inference from inadequate and inaccurate data II, *Proc. Natl. Acad. Sci.*, 65, 281-287.
- Backus, G. E., 1970c. Inference from inadequate and inaccurate data III, *Proc. Natl. Acad. Sci.*, 67, 282-289.
- Backus, G. E. & Gilbert, J. F., 1967. Numerical applications of a formalism to geophysical inverse problems, *Geophys. J. R. astr. Soc.*, 13, 247-276.
- Backus, G. E. & Gilbert, J. F., 1968. The resolving power of gross Earth data, *Geophys. J. R. astr. Soc.*, 16, 169-205.
- Backus, G. E. & Gilbert, J. F., 1970. Uniqueness in the inversion of gross earth data, *Phil. Trans. R. Soc. Lond.*, 266, 123-192.
- Biswas, N. N. & Knopoff, L., 1970. Exact earth flattening calculations for Love waves, *Bull. seism. Soc. Am.*, 60, 1123-1138.
- Bloch, S., Hales, A. L. & Landisman, M., 1969. Velocities in the crust and upper mantle of southern Africa from multi-mode surface wave dispersion, *Bull. seism. Soc. Am.*, 59, 1599-1630.
- Bolt, B. & Dorman, J., 1961. Phase and group velocities of Rayleigh waves in a spherical, gravitating Earth, *J. geophys. Res.*, 66, 2695-2981.
- Crampin, S., 1964. Higher modes of seismic surface waves: Preliminary observations, *Geophys. J. R. astr. Soc.*, 69, 37-57.
- Crampin, S., 1964. Higher modes of seismic surface waves: Phase velocities across Scandinavia, *J. geophys. Res.*, 69, 4801-4811.
- Crampin, S., 1966a. Higher modes of seismic surface waves: Propagation in Eurasia, *Bull. seism. Soc. Am.*, 56, 1227-1239.
- Crampin, S., 1966b. Higher mode seismic surface waves from atmospheric nuclear explosions over Novaya Zemlya, *J. geophys. Res.*, 71, 2951-2958.
- Dahlman, O., 1967a. On Scandinavian crustal travel times. *Försvarets forskningsanstalt. FOA 4 report. C4295-23* Stockholm, 9p.
- Dahlman, O., 1967b. Seismic test explosions in western Sweden, March 1967. *Försvarets forskningsanstalt. FOA 4 report. C4317-20* Stockholm, 11p.
- Davies, D., 1971. Seismology with large arrays (abstract), *EOS, Trans. Am. geophys. Un.*, 52, 280.
- Der, A., Massé, R. & Landisman, M., 1970. Resolution of surface waves at intermediate distance, *J. geophys. Res.*, 75, 3399-3409.
- Derr, J. S., 1969. Free oscillation observations through 1968, *Bull. seism. Soc. Am.*, 59, 2079-2100.
- Dunkin, J. W., 1965. Computation of modal solutions in layered, elastic media at high frequencies, *Bull. seism. Soc. Am.*, 55, 335-358.

- Dziewonski, A. M., 1970. Correlation properties of free period partial derivatives and their relation to the resolution of gross earth data, *Bull. seism. Soc. Am.*, **60**, 741-768.
- Fournier, H. G., 1966. Essai d'un historique des connaissances magnetotelluriques; Note 17, *Inst. Phys. du Globe*, Univ. Paris.
- Fournier, H. G., Ward, S. H. & Morrison, H. F., 1963. Magnetotelluric evidence for the low velocity layer. *Tech. Rept. of Nov. 22 (89)*, Ser. No. 4, Iss. No. 76, *Space Sciences Lab.*, Univ. of Calif., Berkeley.
- Gerver, M. L. & Khazdan, D. A., 1968. Determination of velocity distribution from a dispersion curve, Problems of uniqueness. *Computational Seismology*, No. 4, Nauka (Science) Publishing House, Moscow, 78-94.
- Gregersen, S., 1969. Final report of 16 February 1970; Explosion results. Profile 4-5 Southern Sweden. *Geodetic Institute, Dept. of Seismology*, Copenhagen, Denmark.
- Hales, A. L. & Sacks, I. S., 1959. Evidence for an intermediate layer from crustal structure studies in eastern Transvaal, *Geophys. J. R. astr. Soc.*, **2**, 15-33.
- Haskell, N., 1960. Crustal reflection of plane SH waves, *J. geophys. Res.*, **65**, 4147-4150.
- James, D., 1971. Anomalous Love wave phase velocities, *J. geophys. Res.*, **76**, 2077-2083.
- Landisman, M., Mueller, St & Mitchell, B. J., 1971. Review of evidence for velocity inversions in the continental crust, *American geophys. Union Monograph* 14, J. H. Heacock, ed., in press.
- Lanczos, C., 1956. *Applied Analysis*, Prentice Hall, Englewood Cliffs, N. J., 539 p.
- Mitchell, B. J. & Landisman, M., 1971. Geophysical measurements in the southern Great Plains, *American geophys. Union Monograph* 14, J. H. Heacock, ed., in press.
- Mitchell, B. J. & Landisman, M., 1970.<sup>1</sup> Electrical and seismic properties of the Earth's crust in the southwestern Great Plains of the U.S.A., *Geophysics*, **36**, 363-381.
- Molnar, P. & Oliver, J., 1969. Lateral variations of attenuation in the upper mantle and discontinuities in the lithosphere, *J. geophys. Res.*, **74**, 2648-2682.
- Mueller, St & Landisman, M., 1966. Seismic studies of the Earth's crust in continents I: Evidence for a low-velocity zone in the upper part of the lithosphere. *Geophys. J. R. astr. Soc.*, **10**, 525-538.
- Noponen, I., 1966. Surface wave phase velocities in Finland, *Bull. seism. Soc. Am.*, **56**, 1093-1104.
- Noponen, I., Porkka, M. T., Pirhonen, S. & Luosto, U., 1967. The crust and mantle in Finland, *J. Phys. Earth (Japan)*, **15**, 19-24.
- Press, F., 1966. Seismological information and advances, in *Advances in Earth Science—Internat. Conf.*, Mass. Inst. Tech., 1964, Cambridge, Mass., 247-286.
- Schwab, F. & Knopoff, L., 1970. Surface wave dispersion calculations, *Bull. seism. Soc. Am.*, **60**, 321-344.
- Sellevoll, M. A., 1968. Report on crustal studies in Norway, *Rpt. to U.M.C. Working Group on Explosion Seismology*, Leningrad, 12p., 17 figs.
- Sellevoll, M. A. & Penttillä, E., 1964. Seismic refraction measurements of crustal structure in northern Scandinavia, *Arbok Univ. Bergen, Mat.-Naturv. Ser.*, No. 9, 10p.
- Sellevoll, M. A. & Pomeroy, P., 1968. A travel time study for Fennoscandia, *Arbok Univ. Bergen, Mat.-Naturv. Ser.*, No. 9, 29p.
- Talwani, M., Sutton, G. H. & Worzel, J. L., 1959. Crustal section across the Puerto Rico Trench, *J. geophys. Res.*, **64**, 1545-1555.
- Van Zijl, J. S., 1969. A deep Schlumberger sounding to investigate the electrical structure of the crust and upper mantle in South Africa, *Geophysics*, **34**, 450-462.

- Van Zijl, J. S., Hugo, P. L. V. & De Belloc, J. H., 1970. Ultra Deep Schlumberger sounding and crustal conductivity structure in South Africa, *Geophys. Prosp.*, 18, 615-634.
- Vogel, A. & Lund, C., 1970. Combined interpretation of the trans-Scandinavian seismic profile. Section 2-3. *Report No. 4, Univ. of Uppsala, Dept. of Solid Earth Physics*, 22p.
- Wiggins, R. A., 1968. Terrestrial variational tables for the periods and attenuation of the free oscillations, *Phys. Earth. Planet. Int.*, 1, 201-266.